Chapter 10.   SOLAR ENERGY AND ITS BIOLOGICAL–PHYSICAL INTERACTIONS IN THE SEA

Tommy D. Dickey

University of California, Santa Barbara

Paul G. Falkowski

Rutgers University

Contents

1.   Introduction

For over 4 billion years, solar radiation has played a profound role in driving the physical circulation of the atmosphere, the oceans, and the biological processes responsible for sustaining life on Earth. The angular distribution of, and diel and seasonal changes in, solar radiation are dictated by the relation of Earth's axis to the Sun, the orbital angular velocity of Earth, and the gravitational interactions between Earth, the Sun, and the neighboring planets. To a large extent, these physical interactions are deterministic and have been sustained throughout Earth's history. The angular distribution of radiant energy and the seasonal variations in solar radiation drive large-scale thermohaline circulation of the ocean. This circulation pattern is manifested in an equator-to-pole heat transport superimposed on the surface of a rotating sphere. The meridional transport of heat and formation of deep water at high latitudes are dependent on the angular distribution of solar radiation and continental configuration. On geological time scales there is strong evidence of large thermal changes in both surface and deep waters that clearly must have affected nutrient fluxes, the

depth of the mixed layer, and hence, primary production. For example, stable isotope analyses of oxygen in foraminifera and coccolithophore deposits suggest that bottom waters in the Cretaceous were 10 to 17°C, compared with 2°C at present (Crowley and North, 1991). As surface waters were not significantly warmer than present at low latitudes, the thermal contrast between the surface and deep ocean was much weaker than at present. We are only beginning to understand how these differences in ocean circulation are related to the radiation budget of Earth (Katz et al., 1999), let alone to the biological feedbacks that influence nutrient and biogeochemical cycles. Such understanding can only emerge from interdisciplinary research that accommodates paleo-oceanographic as well as contemporary information. On ecological time scales, the diel and seasonal cycles determine the number of hours of solar radiation incident on each point on the planet, and thus provide an extrinsic natural clock to which almost all organisms (including humans) have adapted. Earth's radiative balance, which is absolutely essential to sustaining life, is dictated by the input of solar energy, atmospheric gas composition, and planetary albedo. These processes are inextricably coupled to the ocean by the hydrological cycle through water vapor and ice albedo feedbacks. These physical systems have coevolved and interact with biological systems. Major biogeochemical processes, such as photosynthesis and nitrogen fixation, are also coupled directly to solar radiation. Solar ultraviolet (UV) radiation can lead to alterations in genetic material, which, in turn, affects the tempo of evolution. Finally, migratory patterns and other behavioral responses in the sea are often keyed to diel, lunar, and seasonal changes in radiation. In this chapter we consider interactions between physical and biological processes in the broad context of how solar radiation drives, selects, and modifies responses in the oceans. Our perspective is based on the overall history of the Earth system, and, in that context, the effects of human activities on Earth's solar radiation budget and its potential impacts on physical and biological processes in the oceans.

2.   Introduction to Relevant Physical
Interactions of Earth with Solar Radiation

Solar energy is produced via proton–proton and higher-order nuclear fusion reactions deep in the Sun's core. The radiation spectrum is dictated to first order by the metalicity, core temperature, and solar mass. The spectral distribution of solar energy closely follows a blackbody curve, with the maximal radiant flux in the visible region of the spectrum (Fig. 10.1). Based on its luminosity and surface temperature, the Sun conforms to a Hertzsprung–Russell (H-R) main star sequence, from which a pattern of solar evolution can be inferred. Based on the H-R sequence, it is estimated that solar luminosity has increased by about 30% since the accretion of Earth. The increased luminosity has been accompanied by small changes in the spectral irradiance. The overall energy budget of Earth is a balance between the input of solar radiation at the top of the atmosphere and its reradiation back to space. The total solar energy flux incident at the top of the atmosphere of Earth is called the solar constant (denoted as S_0). This energy flux is approximately 1360 W m^{-2}, with $S_0/4$ being the proportionate value intercepted by Earth. The fraction of solar radiation reflected back into space is the albedo of Earth, α, which is approximately 0.3. The blackbody radiation emitted by Earth is given by the Stefan–Boltzmann equation, $R = \sigma T^4$, where σ is the Stefan–Boltzmann constant $= 5.67 \times 10^{-8}$ W m^{-2} K^{-4} and T is the temperature
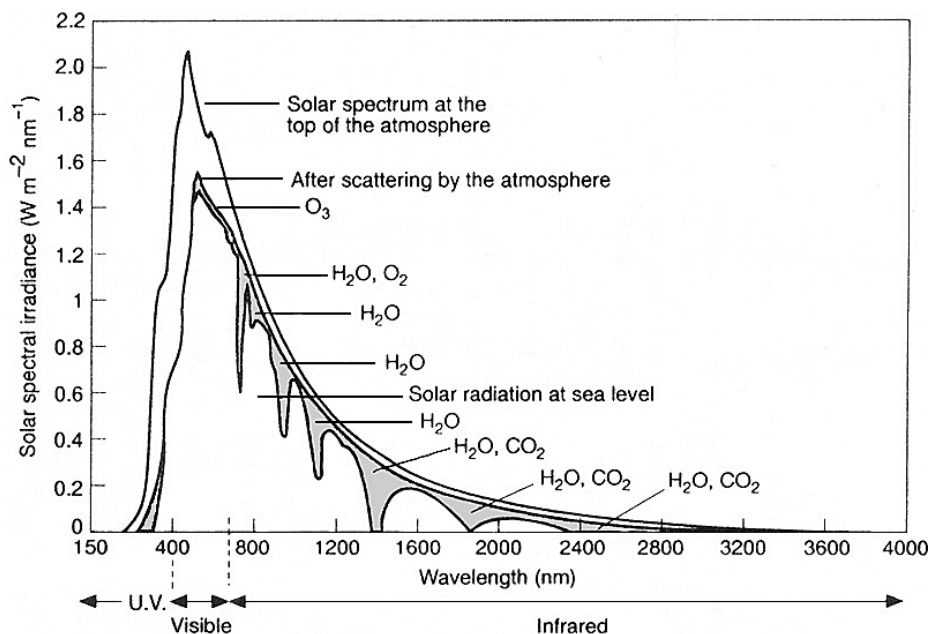
Fig. 10.1.   Spectral distribution of solar radiation at the top of the atmosphere and at sea level. The former follows a blackbody radiation curve, with the maximum radiant energy flux in the visible region of the spectrum. Light impinging on Earth's surface is attenuated by scattering processes in the atmosphere, as well as absorption by gaseous components in the atmospheric column: H_2O, CO_2, and O_3.

of Earth in degrees Kelvin. When Earth is in thermal equilibrium with space, the following balance holds (e.g., Wells, 1997):

$$(S_0/4)(1 - \alpha) = \sigma T^4 \tag{1}$$

From this relation, the average surface temperature should be approximately 255 K; however, the actual temperature is about 286 K. The difference is attributed to the absorption and reradiation of long-wavelength radiation by gases in the atmosphere: the "greenhouse" effect.

   The interaction with and effect of solar radiation on Earth's energy budget is strongly dependent on the electromagnetic spectrum. Planetary albedo is only relevant to short-wavelength radiation; hence, all far-red radiation impinging at the top of Earth's atmosphere will either be absorbed by gases in the atmospheric column or will be transmitted to the surface. Some of the short-wavelength radiation impinging on the top of the atmosphere is scattered and reflected back to space, while the majority penetrates to the surface. Over 70% of Earth's surface is covered by liquid water that absorbs about 95% of incident solar irradiance. In its upper 3 m the ocean contains the equivalent heat capacity of the entire atmosphere of the planet (Peixoto and Oort, 1992). As the average depth of the oceans is about 3800 m, this geophysical fluid acts as a huge heat storage system for the planet. That is, the oceans do not directly affect the radiation budget of the planet, but rather, affect the time constant by which the planet "experiences" changes in radiation.
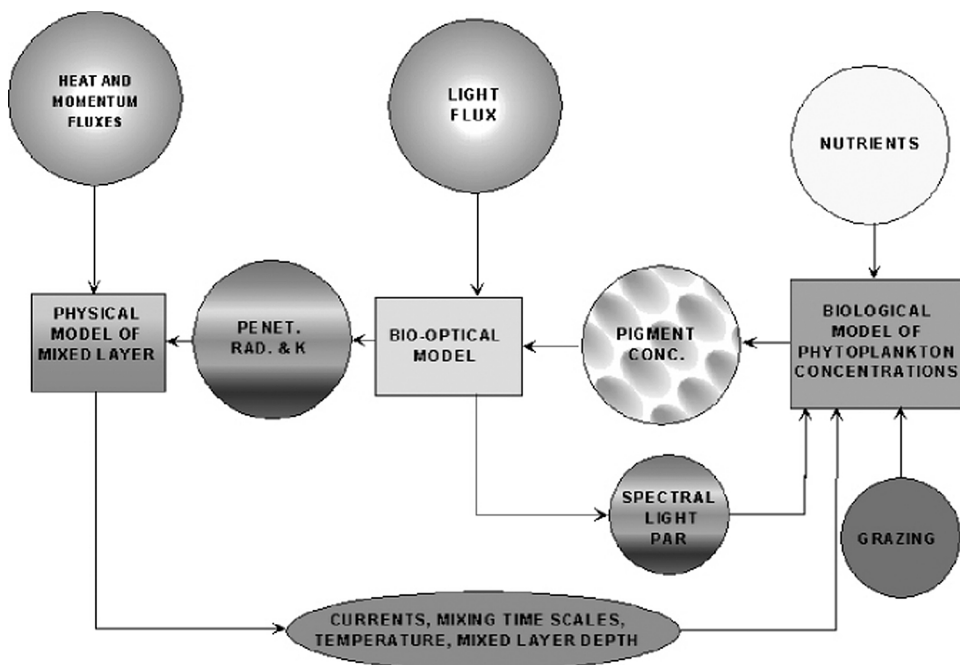
Fig. 10.2. Conceptual model illustrating coupling of physical and biological processes through optical processes. PENET. RAD. and K represent the penetrative component of solar radiation and the diffuse attenuation coefficient of solar radiation. (After Dickey, 1991.)

As in the atmosphere, the direct physical interactions between solar radiation and the ocean are wavelength dependent. Water itself effectively absorbs all incident infrared solar radiation (e.g., Morel and Antoine, 1994), and this direct radiative transfer process provides roughly half of the heat to the ocean surface waters. An example of potential interactions between solar radiation and physical and biological processes is depicted in Fig. 10.2, where the following sequence is illustrated: (1) forcing of the upper ocean physical condition through the input of solar radiation, including light, heat, and indirectly momentum at the ocean surface; (2) upper ocean physical responses, including stratification and turbulent mixing that result in (3) phytoplankton vertical and horizontal motions, which, in turn, lead to (4) feedbacks on distributions of pigments and photosynthetic available radiation (PAR), and (5) modulation of the upper ocean heating via phytoplankton and their associated optical properties. The balance between primary production and grazing determine the concentration of phytoplankton at any moment in time and both processes must be considered in biological–physical interactions.

The interactions among these processes occur on many time and space scales. Long-term changes (millennia to millions of years) in ocean circulation are driven by changes in radiative forcing resulting from orbital variations, albedo feedbacks, and continental configuration (Fig. 10.3). Short-term changes (seconds to decades) are driven by atmospheric conditions (e.g., aerosols, cloud cover, albedo, and ozone concentration) and thermal contrasts between continents and the oceans and from the equator to the poles. Together, both long- and short-term variations in radiative
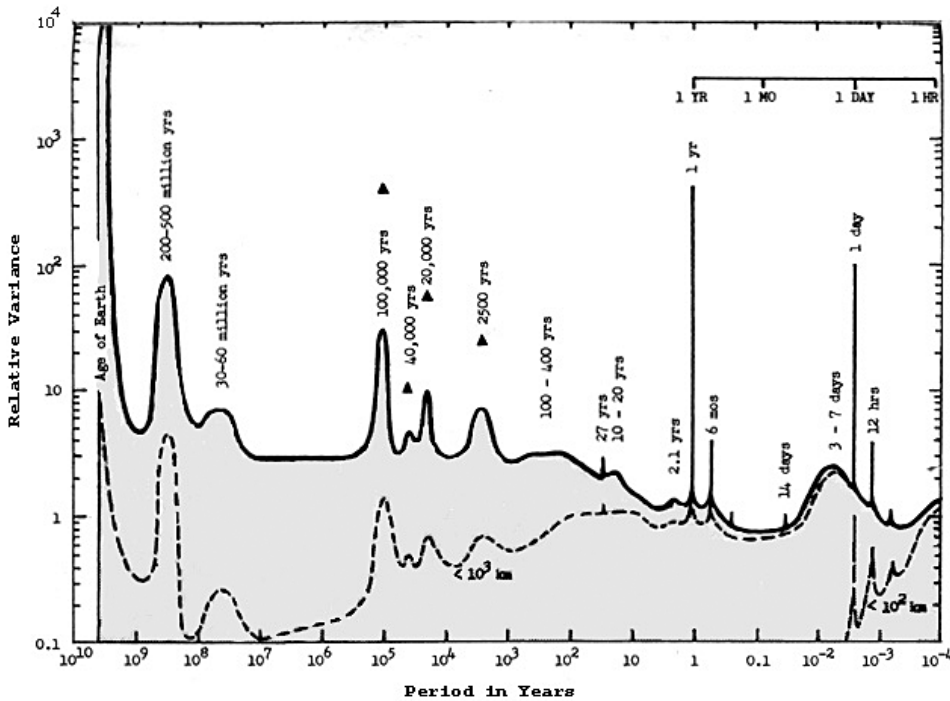
Fig. 10.3. Idealized, schematic spectrum of atmospheric temperature between 10^{-4} and 10^{10} yr. (Adapted from Mitchell, 1976.)

transfer of broadband, as well as visible solar energy, determine the depth of the upper mixed layer, turbulent kinetic energy, and the vigor of large-scale oceanic circulation, which ultimately determines, on a global scale, the distribution and productivity of phytoplankton.

Radiative transfer processes are explicitly dependent on the optical properties of the components in the path between the radiant source (in this case, the Sun), and the radiation sink (the ocean and its constituents). The study of radiative transfer is a branch of oceanography termed *ocean optics*, a term that denotes studies of light and its propagation through the ocean medium. *Bio-optics* invokes the notion of biological effects on optical properties and light propagation, and vice versa (e.g., Smith and Baker, 1978). Excellent references for ocean optics and bio-optics include books by Kirk (1994), Mobley (1994), and Spinrad et al. (1994). The examples of this chapter focus on bio-optical and physical interactions.

Light entering the ocean has only two possible fates; it can be absorbed or scattered. Within this context it is convenient to classify bulk optical properties of the ocean as either *inherent* or *apparent*. Inherent optical properties (IOPs) depend only on the medium and are independent of the ambient light field. The inherent properties include the spectral absorption coefficient $a(\lambda)$, spectral scattering coefficient $b(\lambda)$, beam attenuation coefficient (sometimes denoted as "beam c") $c(\lambda) = a(\lambda) + b(\lambda)$, and spectral single-scattering albedo $\omega_0(\lambda) = b(\lambda)/c(\lambda)$. The proportion of light that is scattered versus absorbed is characterized by $\omega_0(\lambda)$; that is, if scattering prevails,

$\omega_0(\lambda)$ approaches a value of 1, and if absorption dominates, $\omega_0(\lambda)$ approaches 0. Instrumentation has been designed to measure IOPs directly in situ (e.g., Moore et al., 1992; Bruce et al., 1996). These instruments have been deployed from both ship and moored platforms, enabling both high-vertical-spatial and high-temporal-resolution data to be collected and used for studying the interactions between solar energy and physical and biological processes.

IOPs are additive and for many applications, it is often convenient to partition the total absorption coefficient, $a_t(\lambda)$, the total scattering coefficient, $b_t(\lambda)$, and the total beam attenuation coefficient, $c_t(\lambda)$, in terms of contributing constituents. For example:

$$a_t(\lambda) = a_w(\lambda) + a_{\mathrm{ph}}(\lambda) + a_d(\lambda) + a_g(\lambda) \tag{2a}$$

$$b_t(\lambda) = b_w(\lambda) + b_{\mathrm{ph}}(\lambda) + b_d(\lambda) + b_g(\lambda) \tag{2b}$$

$$c_t(\lambda) = c_w(\lambda) + c_{\mathrm{ph}}(\lambda) + c_d(\lambda) + c_g(\lambda) \tag{2c}$$

where subscripts denote contributions by pure seawater (w), phytoplankton (ph), detritus (d), and gelbstoff (g), with units of m^{-1} for all variables. Note that equations 2a to 2c are intended for use where bottom and coastal sediment contributions are minimal. Spectral absorption coefficients have been characterized for pure water by Buiteveld et al. (1994) and Pope and Fry (1997) and for the clearest of natural waters by Smith and Baker (1981). These coefficients are generally considered to be nearly constant in space and time, with greater absorption in the red than the blue portions of the visible spectrum. The shapes and magnitudes of the detrital and gelbstoff absorption spectra can be modeled (e.g., Kirk, 1994) and tend to decrease monotonically with increasing wavelength. Finally, phytoplankton spectral absorption varies significantly in relation to community composition (e.g., Bidigare et al., 1990) and environmental changes, as discussed in the following section. Thus, much bio-optics research focuses on the temporal and spatial variability of $a_{\mathrm{ph}}(\lambda)$. It is worth noting that while ship-based ocean water samples have often been used for studies of the IOPs, it is quite preferable to obtain in situ measurements to ensure realistic local values as well as to characterize temporal and spatial variability. New measurement systems (e.g., Moore et al., 1992; Bruce et al., 1996; Dickey et al., 1998a) are now enabling the collection of $a_t(\lambda)$ and $c_t(\lambda)$ [and by difference, $b_t(\lambda)$]. Using these data and relevant decomposition models (see e.g., Chang and Dickey, 1999), in situ estimates of $a_{\mathrm{ph}}(\lambda)$ and other components (e.g., gelbstoff and colored dissolved organic material, CDOM) can be made for a broad range of environmental conditions as a function of time at fixed depths using moorings (e.g., Chang and Dickey, 2001) or as a function of depth from ships (e.g., Twardowski et al., 1999) or profilers deployed from moorings.

Apparent optical properties (AOPs) depend on both the IOPs and the angular distribution of solar radiation (i.e., the geometry of the subsurface ambient light field). To a reasonable approximation, the attenuation of downwelling incident solar irradiance, $E_d(\lambda, z)$, can be described as an exponential function of depth:

$$E_d(\lambda, z) = E_d(\lambda, 0^-) \exp[-K_d(\lambda, z)\, \Delta z] \tag{3}$$

where z is the vertical coordinate (positive downward), $E_d(\lambda, 0^-)$ is the value of E_d just below the air–sea interface, and $K_d(\lambda, z)$ is the spectral diffuse attenuation coefficient of downwelling irradiance. $K_d(\lambda)$ (here we suppress depth dependence notation for convenience) is one of the important AOPs. The contributions of the various constituents (e.g., water, phytoplankton, detritus, and gelbstoff) to $K_d(\lambda)$ are often represented in analogy to the absorption coefficients given in equation 2a. This leads to the term *quasi-inherent* optical property (e.g., Kirk, 1994), as it is suggestive that inherent optical properties [i.e., like $a_t(\lambda)$] are closely related to $K_d(\lambda)$, which is often described as a quasi-inherent optical property. However, a key point is that $K_d(\lambda)$ is dependent on the ambient light field. It should be noted that for periods of low sun angle and/or when highly reflective organisms or their products (e.g., coccolithophores and coccoliths) are present, multiple scattering becomes increasingly important and simple relations between IOPs and AOPs break down. The relationships between IOPs and AOPs are central to developing quantitative models of spectral irradiance in the ocean. Radiative transfer theory [e.g., reviews by Gordon (1994), Kirk (1994), Mobley (1994), Spinrad et al. (1994)] provides the mathematical formalism for linking IOPs and the conditions of the water environment and light forcing to the radiometry and AOPs of the water column. Spectral radiometric measurements of AOPs are more commonly made than measurements of IOPs.

3. Introduction to Phytoplankton and Their Physiology

On regional and global scales the influence of, and coupling between, physical and biological processes can readily be observed in optical properties from remotely sensed variations in ocean color (Fig. 10.4). Interactions of light with ocean water are described by Maxwell's equations. To first order, a fraction of the visible solar radiation incident on the ocean is scattered back to the atmosphere. Scattering is primarily a consequence of small variations in the refractive index of the water itself, but bubbles play a role as well (Zhang et al., 1998). As a quasi-unstable form of condensed matter, adjacent parcels of water constantly undergo alterations in molecular density, which lead to fluctuations in the refractive index. That is, at any given moment in time, two adjacent parcels of water will contain slightly different numbers of water molecules. This phenomenon is true for any fluid (and glass). The "jumping" of molecules from one parcel to the other leads to *stochastic fluctuations* that produce an incoherence in the optical path of light, resulting in scattering (Einstein, 1910; Mobley, 1994). This fluctuation density scattering function is inversely proportional to the wavelength of light to the 4.3 power. Superimposed on the scattering function is the absorption of light by water, which is much more pronounced in the red than blue and blue-green regions of the spectrum. Hence, to an observer outside the ocean, the upwelling stream of light appears blue, while simultaneously, the wavelengths of light that penetrate deepest into the ocean are blue and blue-green.

The color of the ocean is strongly influenced by suspended particulate materials, dissolved constituents, and bubbles (Kirk, 1992). The absorption and scattering cross sections of each of the components affect the spectral quality of light penetrating through the water column and the upwelling irradiance spectrum. To first order, the photosynthetic pigments of phytoplankton are the major constituents that modify open ocean color from the color blue. These pigments evolved to absorb and trans-
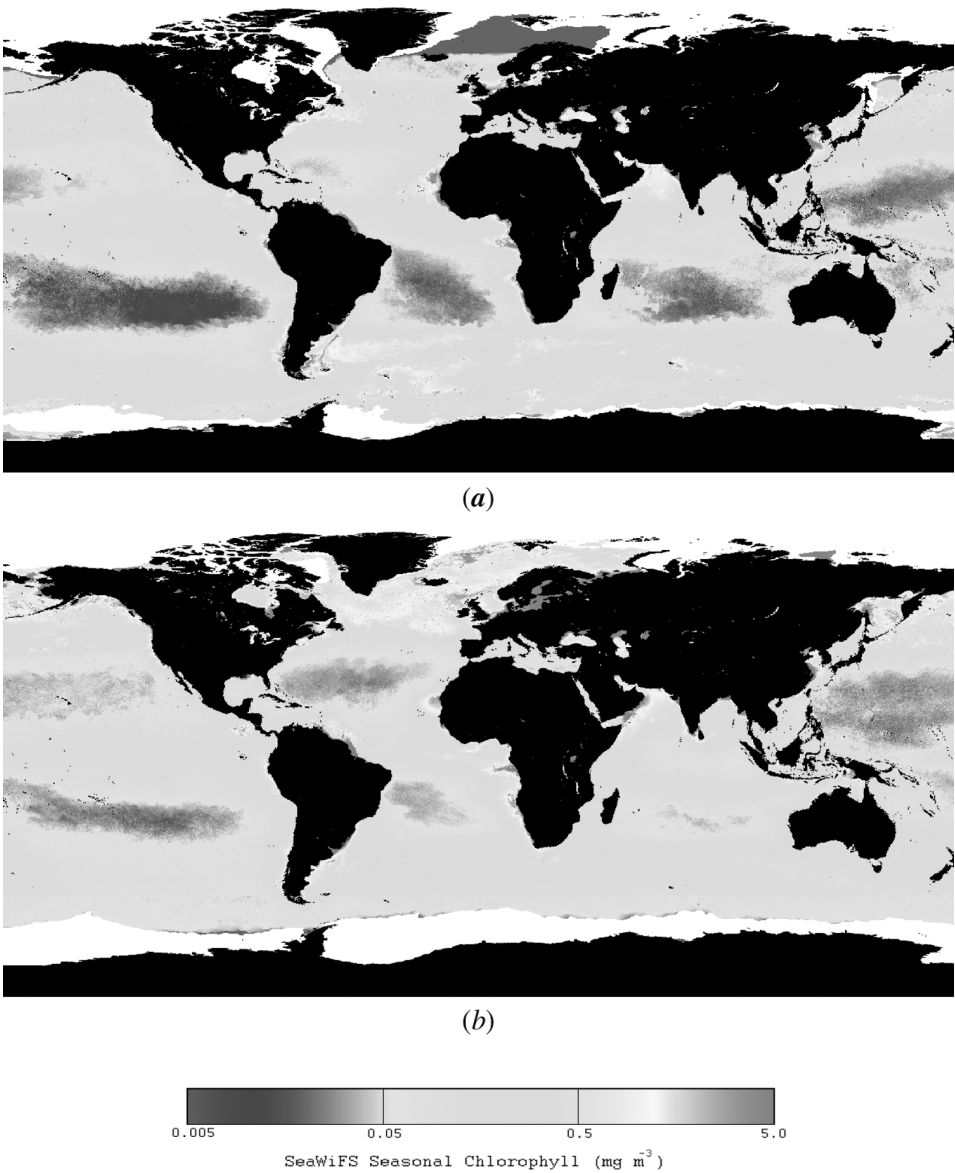
(*a*)

(*b*)

0.005   0.05   0.5   5.0

SeaWiFS Seasonal Chlorophyll (mg m^{-3})

Fig. 10.4.   See color insert. (*a* and *b*) Maps of winter and summer global surface ocean chlorophyll concentrations derived from SeaWiFS measurements of ocean color; (*c* and *d*) corresponding maps of ocean primary productivity derived using the vertically integrated primary production model of Behrenfeld and Falkowski (1997a).

fer light energy to photochemical reaction centers; hence the absorption spectrum of the pigments often overlaps the maximum spectral irradiance in the ocean (Yentsch, 1960, 1980). Specifically, the blue and blue-green downwelling and upwelling photons are absorbed by the Soret absorption bands of chlorophylls and carotenoids as chlorophyll *a* and its divinyl derivative are present in all oxygen-producing photo-
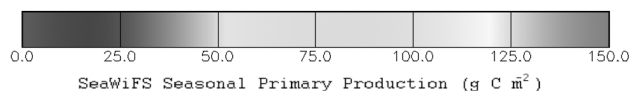
(*c*)

(*d*)

0.0   25.0   50.0   75.0   100.0   125.0   150.0
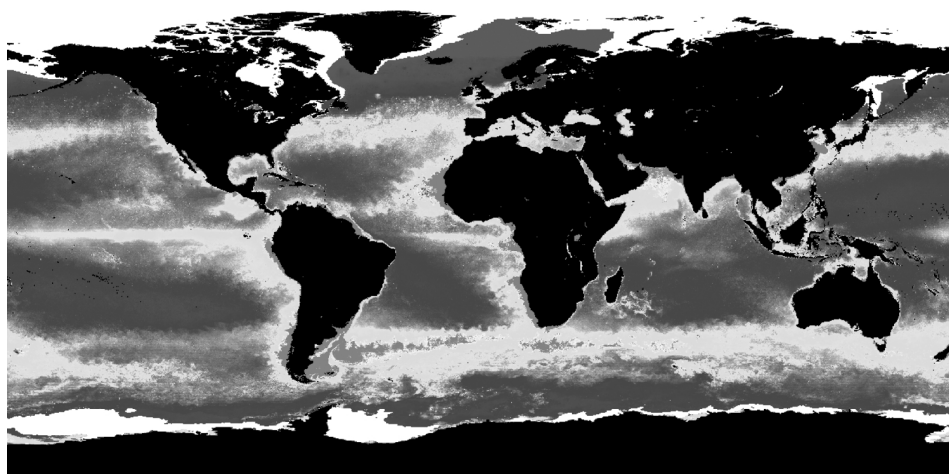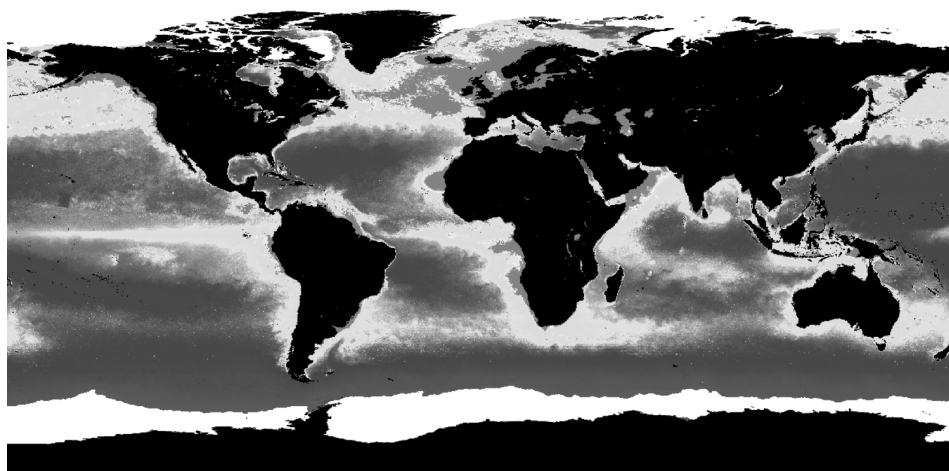
SeaWiFS Seasonal Primary Production (g C m^2)

Fig. 10.4.   Continued.

synthetic organisms (Falkowski and Raven, 1997). In the presence of photosynthetic organisms, the upwelling and downwelling irradiance stream becomes depleted of blue and blue-green light; in effect, the water becomes "darker." The depletion of light in these wavelengths is, in the open ocean, quantitatively proportional to the concentration of photosynthetic pigments in the optical path (i.e., the upper portion of the euphotic zone). Using the ratio of two wavelengths of light, it is possible to determine the water-leaving radiances $L_w(\lambda)$ empirically (i.e., the photons scattered by the ocean back to the atmosphere) to estimate phytoplankton pigment concen-

trations. The pigment concentrations are usually reported in terms of chlorophyll *a* (although the assumption that the water-leaving radiance is actually quantitatively related to chlorophyll *a* is generally overly optimistic). Also, bubbles can shift ocean color toward the green, which introduces errors in remote sensing of phytoplankton (Zhang et al., 1998).

The mean circulation of the upper ocean provides a driving force for nutrient fluxes, either from coastal upwelling or geostrophic forcing on the gyre boundaries. In general, the advective supply of nutrients potentiates the growth and accumulation of phytoplankton biomass, which can be detected from satellite imagery of changes in ocean color (Fig. 10.4). While such imagery can be quantitatively informative, the qualitative patterns are remarkable in their correspondence to physical circulation, as revealed, for example, by altimetry and sea surface temperature (Fig. 10.5). Time series of satellite imagery reveal the periodic and episodic blooms of phytoplankton in temperate and boreal ocean regions (Fig. 10.4) that are tied to the ability of cells to utilize the available nutrients. In such regions, nutrient drawdown is related to the ratio of the upper mixed layer to the depth of the euphotic zone (i.e., the critical depth) and insolation. The effect of interannual variations in sea surface temperature (e.g., due to El Niño events) on phytoplankton abundance can also be discerned as primarily influencing the infusion of nutrients into the upper mixed layer. Although the estimate of phytoplankton biomass from satellite imagery is indirect and limited to the upper portion of the euphotic zone, statistical distributions can be used to infer both light penetration through the euphotic zone as well as the vertical structure of the phytoplankton community (Morel and Berthon, 1989). In regions far removed from continental sources of nonbiological particles (e.g., the central ocean basins), deviations in ocean color from pure seawater are influenced primarily by biologically derived materials, of which the most important are pigmented phytoplankton. The particle-size spectrum in the tropics and subtropical gyres is highly skewed toward small cells (the picoplankton; scale less than 2 μm). These small cells have relatively large scattering cross sections (Stramski and Kiefer, 1991). Bubbles, introduced primarily by breaking waves, also contribute to scattering (but not spectral absorption). Hence, by assuming that the pigments are contained within such cells, it is possible to calculate via a simple radiative transfer model, the spectral absorption of light through the water column, thereby deriving an estimate of euphotic zone or depth. In the simplest model, the biomass is assumed to be uniformly distributed throughout the euphotic zone (i.e., the contribution of the pigmented cells to the absorption of light is constant). In reality, chlorophyll concentrations almost always increase toward the base of the mixed layer. The increase in chlorophyll is a consequence of both physiological acclimation to lower irradiance and the availability of nutrients near the base of the mixed layer (e.g., Cullen, 1982). The increase in chlorophyll often does not represent an increase in phytoplankton biomass (i.e., the ratio of cell carbon to chlorophyll decreases) (Falkowski, 1983; Olson et al., 1990). Based on thousands of vertical profiles of chlorophyll biomass throughout the oceans, Morel and Berthon (1989) developed a statistical climatology that relates the satellite-based estimate of chlorophyll (i.e., that inferred for the upper portion of the euphotic zone) to the vertical distribution of chlorophyll biomass (Fig. 10.6). By using such a model, it is possible to infer the spectral irradiance at any depth within the euphotic zone for a nonuniform chlorophyll distribution.

Finally, satellite data sets of chlorophyll biomass have been used to derive regional
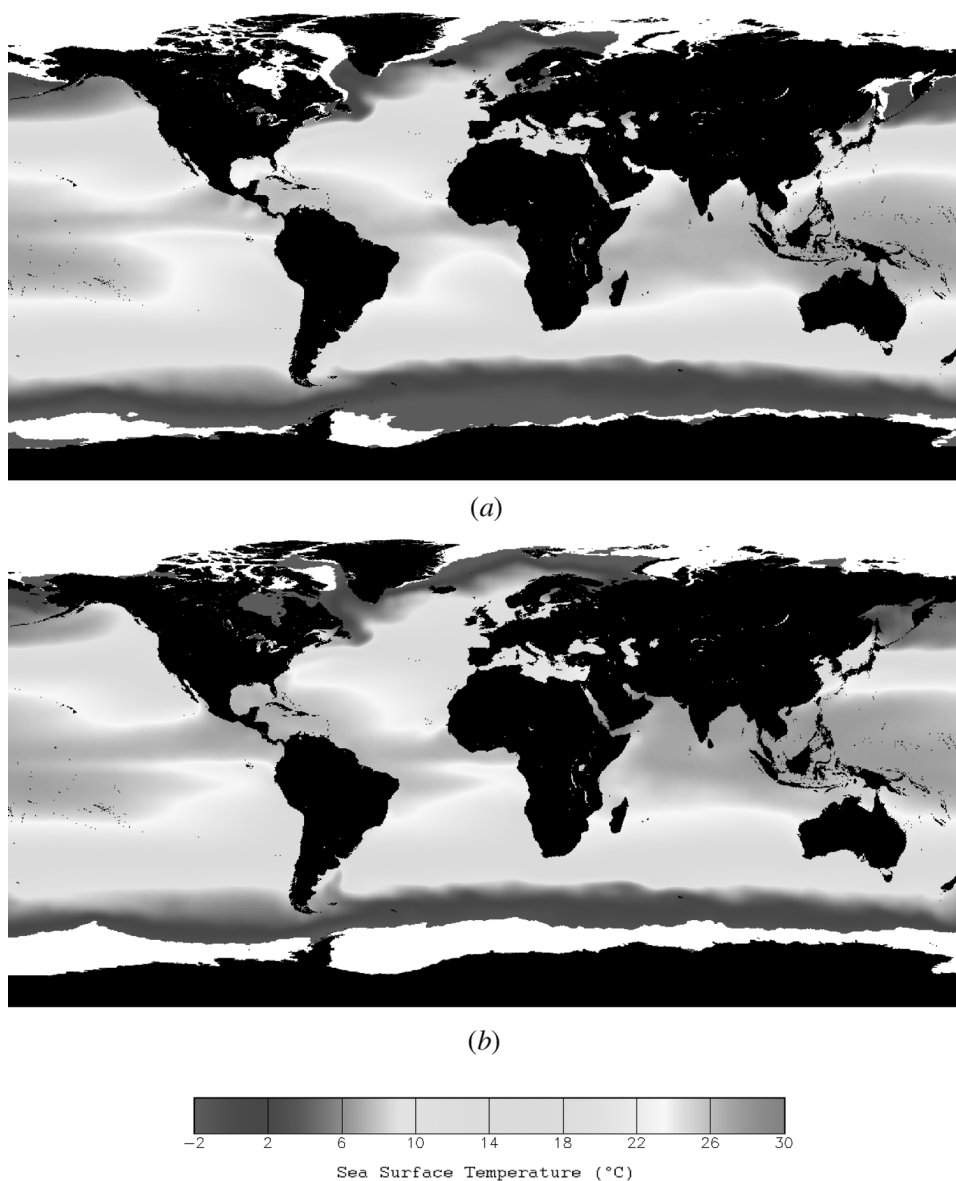
Fig. 10.5. See color insert. (*a*) Winter and (*b*) summer global maps of sea surface temperature.

and global estimates of primary production based on models (Fig. 10.4). Although there are myriad papers describing various approaches to estimate primary production, the models can be classified in a simple hierarchy depending upon the level of mathematical integration that is used. Behrenfeld and Falkowski (1997a) describe four basic model schemes (Table I), all of which can be related to each other mathematically. This topic is discussed later.

(a)

(b)
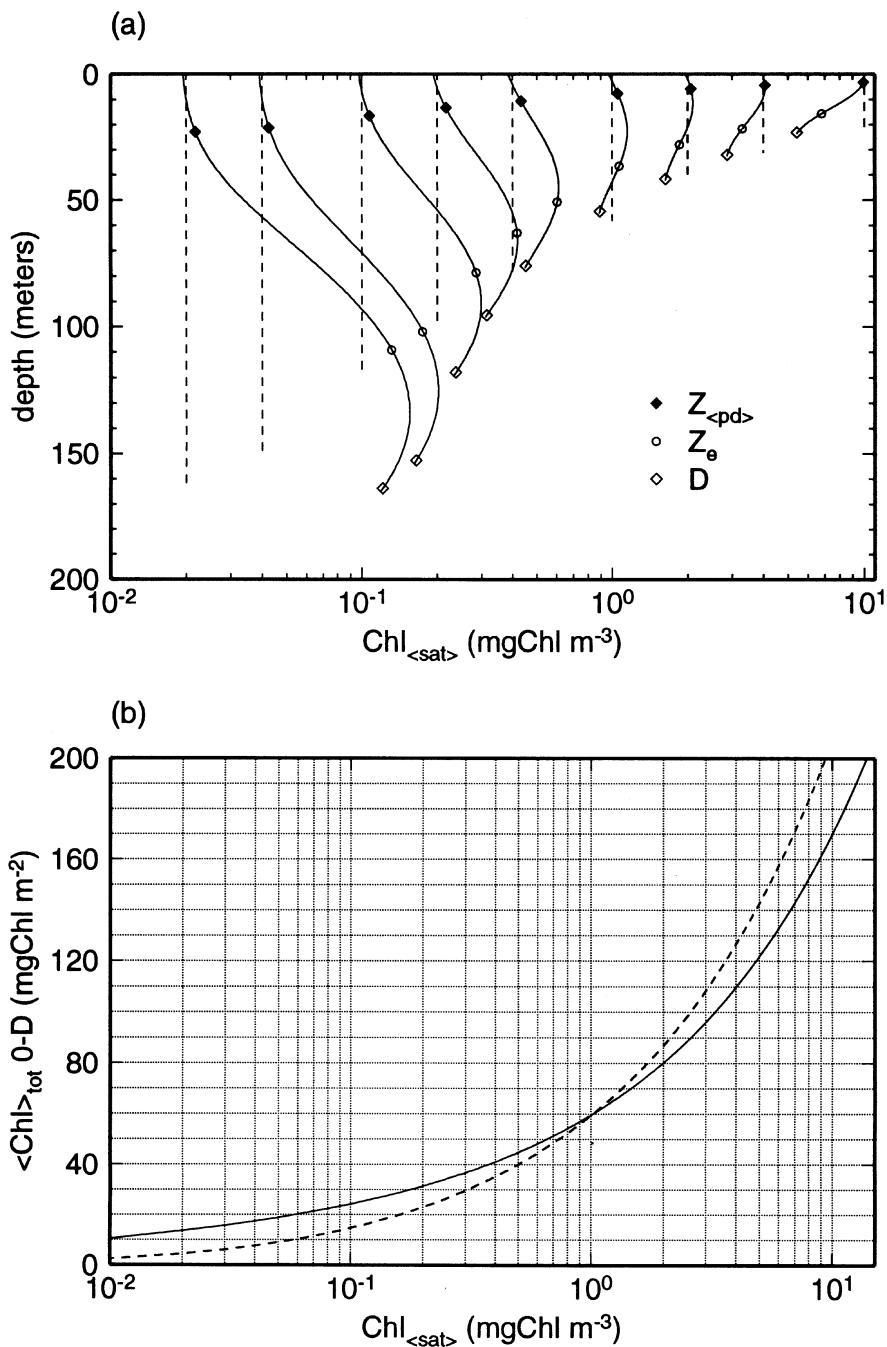
Fig. 10.6. (*a*) Vertical profiles of chlorophyll as a function of chlorophyll concentration based on a statistical analysis (Morel and Berthon, 1989) and assuming a homogeneous distribution (dashed line); (*b*) relationship between the surface ocean chlorophyll concentration as inferred from satellite data (e.g. Fig. 10.4*a* and *b*), and the water column integrated value given the statistical distribution above (solid line) and a homogeneous distribution (dashed line). D, day length; Ze, euphotic zone.

TABLE I

Classification System for Daily Net Primary Productivity (NPP) Models
Based on Implicit Levels of Integration[a]

I. Wavelength-resolved models (WRMs)

$$NPP = \int_{\lambda=400}^{700} \int_{t=sunrise}^{sunset} \int_{z=0}^{Z_{eu}} \Phi(\lambda, t, z) \cdot PAR(\lambda, t, z) \cdot a^*(\lambda, z) \cdot Chl(z) \, d\lambda \, dt \, dz - R$$

II. Wavelength-integrated models

$$NPP = \int_{t=sunrise}^{sunset} \int_{z=0}^{Z_{eu}} \varphi(z, t) \cdot PAR(t, z) \cdot Chl(z) \, dt \, dz - R$$

III. Time-integrated models

$$NPP = \int_{z=0}^{Z_{eu}} P^B(z) \cdot PAR(z) \cdot DL \cdot Chl(z) \, dz$$

IV. Depth-integrated models

$$NPP = P^B_{opt} \cdot f[PAR(0)] \cdot DL \cdot Chl \cdot Z_{eu}$$

Source: Behrenfeld and Falkowski (1997a).

[a]Each category includes a photoadaptive variable [i.e., φ, Φ, $P^B(z)$, P^B] corresponding to the resolution of the described light field. The variables Φ and φ are chlorophyll-specific quantum yields for absorbed and available photosynthetically active radiation, respectively. Wavelength-resolved models and wavelength-integrated models are parameterized using measurements of net photosynthesis and require subtraction of daily photoautotrophic respiration (R) to calculate NPP. $P^B(z)$ and P^B_{opt} are chlorophyll-specific rates obtained from measurements of daily primary production and thus do not require subtraction of respiration. DL, day length (hours).

4. Examples of Biological–Physical Coupling Influenced by Light

4.1. *Variability of Inherent Optical Properties*

The observed temporal and spatial variabilities of bulk inherent optical properties (IOPs), such as the total absorption and scattering coefficients, $a_t(\lambda)$ and $b_t(\lambda)$, are caused by physical, chemical, and biological processes. For example, water parcels, which encompass particulate and dissolved materials, move in response to physical forcing over a broad spectrum of time and space scales (e.g., covering over 10 orders of magnitude; see Dickey, 1991): small-scale molecular and turbulent motions (millimeters to centimeters) to frontal and mesoscale eddy scales (roughly tens of kilometers to 200 km) to gyre scales (thousands of kilometers). Processes such as advection and mixing are important for redistributing IOPs, but there is more to the story, as IOPs are not strictly conservative. If IOPs were, we would expect to be able to trace their distributions as we do salinity. However, it has been suggested that dissolved and particulate materials may be used as approximate passive tracers of water masses under particular circumstances and over limited time and space scales (e.g., Pegau, personal communication). To explore this interesting prospect, each IOP component needs to be considered. The variability in the absorption and scattering coefficients of pure ocean water, $a_w(\lambda)$ and $b_w(\lambda)$ are usually considered to be invariant in the upper ocean, and much effort has been made to determine these values to a high accuracy (Smith and Baker, 1981; Buiteveld et al., 1994; Pope and Fry, 1997). Variability due to gelbstoff or colored dissolved organic material (CDOM), as represented in absorption coefficients, $a_g(\lambda)$, can be great in nearshore waters because of terrigenous sources as discussed earlier. The dynamic range of variability in $a_g(\lambda)$ is considerably smaller in the open ocean. However, it has been reported that on seasonal time scales (with depth dependence as well), the variability in a related quantity, diffuse light attenuation coefficient due to both CDOM and detrital materials (CDM)

or K_{cdm} (440 nm), is quite significant in the Sargasso Sea and needs to be included in remote sensing estimates of chlorophyll a (Siegel and Michaels, 1996; Nelson et al., 1998). The dissolved component property [as characterized by say $a_g(\lambda)$] is generally expected to act more like a "conservative" tracer than the particulate component. Summertime photo-oxidation of the dissolved material near the surface causes removal of the labile portion leaving the longer-lasting refractory component (e.g., Vodacek et al., 1997), so that $a_g(\lambda)$ can in principle act quite well as a conservative tracer (Pegau, personal communication) at least over limited time scales.

In the open ocean, changes in bio-optical properties reflect changes in phytoplankton community (species) structure and/or physiological state. The time scales of these changes can range from minutes to several days to seasons (Falkowski, 1984). External forcing mechanisms include surface waves and clouds, diurnal and seasonal solar cycles, and wind and mesoscale events. High-frequency in situ measurements of bio-optical and chemical parameters [PAR, beam c, chlorophyll fluorescence (discussed in detail below), and dissolved oxygen] have suggested that rapid photoacclimative responses (on the order of tens of minutes) can take place in a phytoplankton community (e.g., Owens et al., 1980; Abbott et al., 1982; Stramska and Dickey, 1992a, 1998). Diel variability has also been clearly seen in several bio-optical and chemical time series (e.g., Siegel et al., 1989; Hamilton et al., 1990; Cullen et al., 1992; Stramska and Dickey, 1992b; Kinkade et al., 1999). The diel signal can result from physical processes such as changes in particle concentrations related to diel mixed layer depth variability (e.g., Gardner et al., 1995) and from changes in phytoplankton physiology and chemical composition (e.g., Cullen and Lewis, 1995; Stramski et al., 1995; DuRand and Olson, 1996). The attenuation of a coherent light beam is a function of the number of absorbing molecules as well as the concentration of particles and the scattering cross section of particles in the beam's path. Cell division in almost all phytoplankton taxa is keyed to a circadian rhythm, such that there is a diel cycle in cell size that results from the division cycle (Chisholm et al., 1980; Vaulot and Partensky, 1992). Changes in cell size affect the backscatter cross section (van de Hulst 1981), where the smaller the particle, the larger the scattering cross section. This effect can be visualized intuitively by considering the scattering function of glass; a drinking glass, which is macroscopic, is basically transparent (low scattering cross section). If one crushes the glass to smaller and smaller particles, the ensemble of particles no longer is clear, but rather, appears to be a white powder (large scattering cross section). Thus, the same amount of material can scatter more or less light, depending on the size. The scattering function is further influenced by the refractive index (Morel, 1991). During the photoperiod, phytoplankton tend to accumulate carbohydrates and/or lipids as the immediate storage product of photosynthesis; this carbohydrate is consumed at night to form protein (Cuhel, 1984; Post et al., 1985; Falkowski, 1997). The accumulation of carbohydrates and lipids leads to changes in the refractive index (Morel, 1991), which, in turn, affects the scattering efficiency of a coherent beam. Finally, changes in the chlorophyll content per cell are an inevitable outcome of phased cell division in a synchronized phytoplankton assemblage. Thus, when cell division occurs, the concentration of chlorophyll per unit cell volume generally increases (chloroplast volumes do not change as markedly as total cell volumes), leading to alterations in the "package" or "sieve" effect (Duysens, 1956; Latimer and Rabinowitch, 1959). The latter changes influence both the optical absorption cross section and the fluorescence efficiency in a diel cycle.

A diel cycle has been entrained in virtually all procaryotic (Mori et al., 1996) as well as eucaryotic (including human) genetic systems (Takahashi, 1992). Such "clock genes" provide cells information critical to coordination of the assimilation of nitrogen and carbon (Carpenter et al., 1992; Ramalho et al., 1995), protein synthesis (Milos and Hastings, 1990), as well as cell cycling (Chisholm et al., 1980). The phylogenetic conservation of the clock genes is remarkable and bespeaks a strong evolutionary selection pressure to force biological systems to conform to solar energy variations on the diel scale. The evolution of signal molecules in photoautotrophic organisms to further "count" the number of hours in the day resulted in a second set of gene sequences that keeps track of seasons in higher plants, with clear genetic roots in cyanobacterial chromophores (Hughes and Lamparter, 1999).

One of the most sensitive signatures of phytoplankton optical properties is chlorophyll fluorescence. The coloration of phytoplankton is a consequence of evolutionary selection of pigments that can absorb and transfer excitation energy to photosynthetic reaction centers, where the excitation energy (in the form of an "exciton," an excited state within a lattice structural matrix) can be used to induce physical charge separation. Phytoplankton comprises at least eight taxonomic divisions (the equivalent of animal phyla), each of which has one or more distinctive light-harvesting pigments. Excitation energy is transferred from pigment to pigment within a protein scaffold via either Förster resonance or excitation coupling (Falkowski and Raven, 1997). The excitation transfer almost always proceeds "downhill" (i.e. to longer-wavelength pigments). The terminus of excitation transfer is chlorophyll a, from whence a fraction of the excitation energy is emitted to the environment in the red portion of the spectrum (centered at 683 nm). In vivo, chlorophyll fluorescence competes for excitons with two other energy-dissipating processes, photochemistry and nonradiative energy dissipation (heat). As such, it is possible to relate changes in chlorophyll fluorescence quantitatively to the quantum yield of photochemistry, and instrumentation for such measurements is commercially available (Neubauer, 1993; Kolber et al., 1998).

Formally, when phytoplankton are placed in darkness and exposed to a weak flash of light, the fluorescence yield obtained is at a minimum, or F_0 level. Following exposure to a light sufficiently intense to reduce all the primary electron acceptors, the fluorescence yield rises to a maximum, or F_m, level. The difference, $F_m - F_0$, is called "variable" fluorescence, and when normalized to F_m is quantitatively related to the photochemical efficiency of photosynthesis (Butler, 1972).

By following changes in variable chlorophyll fluorescence in situ over large swaths of ocean surface waters, it is possible to observe large-scale variations in the quantum yield of photochemical energy conversion efficiency in phytoplankton. The changes in yields are associated with two major physical processes, incident solar radiation and turbulent mixing. We consider these in turn.

In all natural phytoplankton communities, there is a strong diel component to the fluorescence signal. Normally, fluorescence normalized per unit chlorophyll a (i.e., the fluorescence yield) is attenuated in midday, when solar radiation is highest (Owens et al., 1980). This attenuation has two components. One component is related to the photochemical energy conversion process itself. If measured with an instrument containing a light source that induces the fluorescence in the ambient light, the "stimulated" or "active" fluorescence is superimposed on a solar-induced fluorescence profile. Thus, the stimulated fluorescence measures a component of variable fluorescence that can be induced over and above that of the sun (Falkowski and Kolber, 1995). As

photochemical reactions of photosynthesis are light saturable, when background irradiance increases, there is a decreased probability of finding an "open" photochemical target or "hole" for absorbed radiation. Thus, the change in fluorescence induced by an actinic source also decreases. This process is called photochemical quenching.

The photochemical target for excitation energy can be inferred from the rate of light saturation of fluorescence. This saturation profile, described by a cumulative one-hit Poisson function, reflects the effective absorption cross section for the photochemical reaction (Ley and Mauzerall, 1982; Falkowski and Kolber, 1995). All photosynthetic organisms have developed mechanisms to adjust these cross sections dynamically in response to background light (Long et al., 1994). Thus, as irradiance increases, the cross section can be made smaller to minimize photodamage to the reaction centers; conversely, when irradiance decreases, the cross sections can be made larger, to optimize light harvesting. There are two major strategies for altering cross sections. On short time scales (minutes), the adjustments are made by adding or removing pigments that dissipate the excitation as heat. These pigments, a set of taxonomically dependent carotenoids, are located within the light-harvesting systems and compete effectively with chlorophyll *a* for fluorescence. Thus, when irradiance is high, there is an overall reduction in fluorescence yield, reflecting a decrease in the effective cross section of the photochemical process (Olaizola et al., 1994). The reduction in fluorescence is a component of what is sometimes called nonphotochemical quenching (Falkowski and Kolber, 1995). On longer time scales, cells can increase or decrease the number of chromophores per unit cell through a feedback process coupled to sense irradiance levels (Escoubas et al., 1995).

Superimposed on the diel changes in fluorescence are short-term variations resulting from the passage of clouds across the sky and photodamage to the reaction centers resulting from overexposure to supraoptimal irradiance. The passage of clouds across the sky is slow enough to permit changes in the effective cross sections of the photosynthetic apparatus, leading to a change in fluorescence yields. This phenomenon is readily observed in stimulated fluorescence profiles or time series made under partially cloudy conditions (e.g., Abbott et al., 1982; Stramska and Dickey, 1992a, 1998). Under high irradiance levels, a fraction of the photochemical reaction centers can become "irreversibly" damaged; repair is accomplished by de novo protein synthesis. The damaged reaction centers act as nonphotochemical fluorescent quenchers, but recovery occurs on time scales of hours. Depending on the availability of nutrients (which are essential for protein synthesis), total repair is usually achieved overnight.

Physical turbulence is a primary mechanism responsible for bringing nutrients into the euphotic zone. Under nutrient-replete conditions, the maximum change in variable fluorescence is remarkably constant for a wide number of phytoplankton taxa (Kolber et al., 1988). As cells become nutrient limited, however, the quantum yields decline. Transects of variable fluorescence signals show large-scale variations in fluorescence yields that correspond to changes in water mass characteristics, especially to nutrient supply. Thus, as physical fronts or eddies develop, the associated changes in nutrient supply are manifested in photochemical energy conversion efficiency. The sensitivity and precision of variable fluorescence measurements can be used to infer mesoscale physical–biological interactions in real-time as well as from moored instrumentation.

The diel cycle is critically important as an evolutionary selection process in both phytoplankton and zooplankton in the context of vertical migrations. Because solar energy inputs are required for photosynthesis, yet lead simultaneously to stratification,

nutrient supplies in the euphotic zone can be depleted while light is still plentiful. Some taxa of phytoplankton have developed vertical migration strategies to acquire nutrients at night while optimizing light harvesting for carbon fixation during the day. These taxa include cyanobacteria, dinoflagellates, diatoms, and chlorophytes. The migratory patterns are manifested as changes in the distribution of optical properties in the euphotic zone, and can be disrupted or modified by turbulent mixing. The vertical migration of zooplankton, keyed to resource acquisition and predator avoidance, is a higher level of behavioral response that involves direct light perception (vision) and phototaxis (Forward, 1988).

The seasonal cycles of phytoplankton and zooplankton at temperate to high latitudes have been of interest to biological oceanographers since the 1920s. An historical development of explanations for these cycles may be found in Mann and Lazier (1991). Perhaps the most studied aspect has been the spring phytoplankton bloom phenomenon, which progresses in time toward higher latitudes from spring to summer and is especially dramatic in the North Atlantic, as evidenced in ocean color imagery (Fig. 10.4). The classical explanation of the seasonal spring bloom was apparently first forwarded by Gran (1931) and later placed on a theoretical basis by Sverdrup (1953). A brief description of the Northern Hemisphere's spring bloom and seasonal cycle follows [see Mann and Lazier (1991) for details]. First, the winter is characterized by low populations of phytoplankton, despite high availability of nutrients by deep mixing, with community respiration exceeding photosynthesis because the phytoplankton's vertical excursions take them well below the euphotic zone (note that daily integrated light is also minimal during this season). Then, with spring stratification of the upper layer, the vertical motions of phytoplankton are restricted to the upper layer, which is still replete with nutrients, where they receive sufficient light (light is now more available) for photosynthesis to exceed respiration and grazing loss. This results in large-scale reproduction and blooms. The ensuing strong seasonal stratification of the pycnocline (thermocline) then acts as a barrier to the influx of nutrients from depth, and thus the phytoplankton in the mixed layer (and euphotic layer) eventually deplete the requisite nutrients. Reduced phytoplankton concentrations in the upper layer are also caused by the sinking of phytoplankton and grazing by zooplankton. The end of the spring bloom is then characterized by low concentrations of phytoplankton and nutrients in the upper layer. The early summer period is marked by a subsurface chlorophyll maximum (not visible from airplane and satellite color sensors), which is often near the bottom of the euphotic zone (nominally, the depth where light is reduced to 1% of its surface value) and in the upper thermocline/pycnocline for reasons described earlier (e.g., see also Cullen, 1982). The chlorophyll maximum is often somewhat below the depth of maximum primary productivity, with both regions contributing significantly to the depth of integrated primary production (e.g., Hayward and Venrick, 1982). During some years and in some locations, a fall bloom occurs as the mixed layer deepens to sufficient depths to entrain nutrients into the upper layer, where daily light is still sufficient for photosynthesis. This general depiction of the seasonal cycle appears to be well supported by several experiments which have used monthly interval shipboard sampling or more recently, high temporal resolution sampling of physical, chemical, and bio-optical variables (e.g., Sargasso Sea: Smith et al., 1991; Marra et al., 1992; Dickey et al., 1993a, 1998a).

Although the seasonal cycle is a very dominant signal, high-temporal-resolution time series have revealed considerable complexity in the phytoplankton biomass

and primary production and show that aliasing can be problematic for coarse (monthly) sampling (e.g., Wiggert et al., 1994). As described earlier, short time-scale variations in phytoplankton populations are caused by passages of clouds and the diel solar cycle. In addition, short-lived blooms and busts (cessations of blooms) are especially evident in the springtime when shallow mixed layers are often formed and then erased because of wind events (e.g., Dickey et al., 1991, 1993a, 1998a), as shown in Figure 10.7. In particular, a set of observations in the open ocean south of Iceland (Dickey et al., 1994) showed that even modest near-surface stratification, preceding formation of the seasonal thermocline, can be sufficient to initiate shallow phytoplankton blooms, which can in turn intensify near-surface heating rates and stratification (Stramska and Dickey, 1993, 1994). These types of observations and sequences of ocean color observations from space suggest that the integrated effect of the phytoplankton seasonal cycle and its poleward march are built on many cumulative events driven by short time- and space-scale forcing as well as the periodic seasonal solar insolation.

Energetic mesoscale features (e.g., fronts, eddies, and rings) further complicate a simple seasonal description and modeling of phytoplankton. In particular, eddies can introduce nutrient-rich waters into the euphotic layer, where they can drive phyto-plankton productivity (e.g., Falkowski et al., 1991; Dickey et al., 1993a). In the Sargasso Sea, the influence of eddies on new production (i.e., the fraction of total primary production in surface waters fueled by externally supplied nutrients) is well documented (McGillicuddy et al., 1998; McNeil et al., 1999). This problem was attacked using high-resolution physical, bio-optical, and chemical measurements from a mooring, ship survey data, satellite altimetry data, and eddy-resolving model simulations. The vertical transport of nutrients into the euphotic layer, along with elevated levels of chlorophyll, are apparent in the time series shown in Fig. 10.7 as a second baroclinic mode eddy passed the Bermuda Testbed Mooring (BTM) in July 1995. It is interesting to note that near-inertial oscillations (inertial period of about 22.8 h) are superimposed on the dominant eddy signature. These observations suggest that in addition to seasonal convection, mesoscale eddies can make major contributions to the vertical flux of nutrients into the euphotic zone and may be sufficient to balance the annual nutrient budget of the region and account for discrepancies in regional estimates of new production (McGillicuddy et al., 1998; McNeil et al., 1999). In separate but related work, Granata et al. (1995) have reported increased subsurface chlorophyll concentrations, which were observed as near-inertial waves propagated along a front in the Sargasso Sea, suggesting that shear instabilities associated with the wave packets stimulated new production.

The seasonal cycle of bio-optical properties of the coastal ocean has been observed to follow a pattern similar to that of the open ocean by several studies (e.g., Chang and Dickey, 2001). However, the coastal environment is far more complex because of several factors, such as terrigenous input of materials as described earlier, bottom boundary layer effects, resuspension of bottom materials, greater roles of tides and internal solitary waves, topographically related fronts, and water mass intrusions (e.g., from impinging eddies). In addition, major events such as hurricanes can rapidly modify the ecosystem and optical properties (e.g., Dickey et al., 1998c, d). It is interesting to note that bottom sediments were suspended more than 30 m above the ocean bottom (about 70 m depth) during the passage of Hurricane Edouard at a mooring site located about 110 km south of Cape Cod, Massachusetts. A time series of spectral
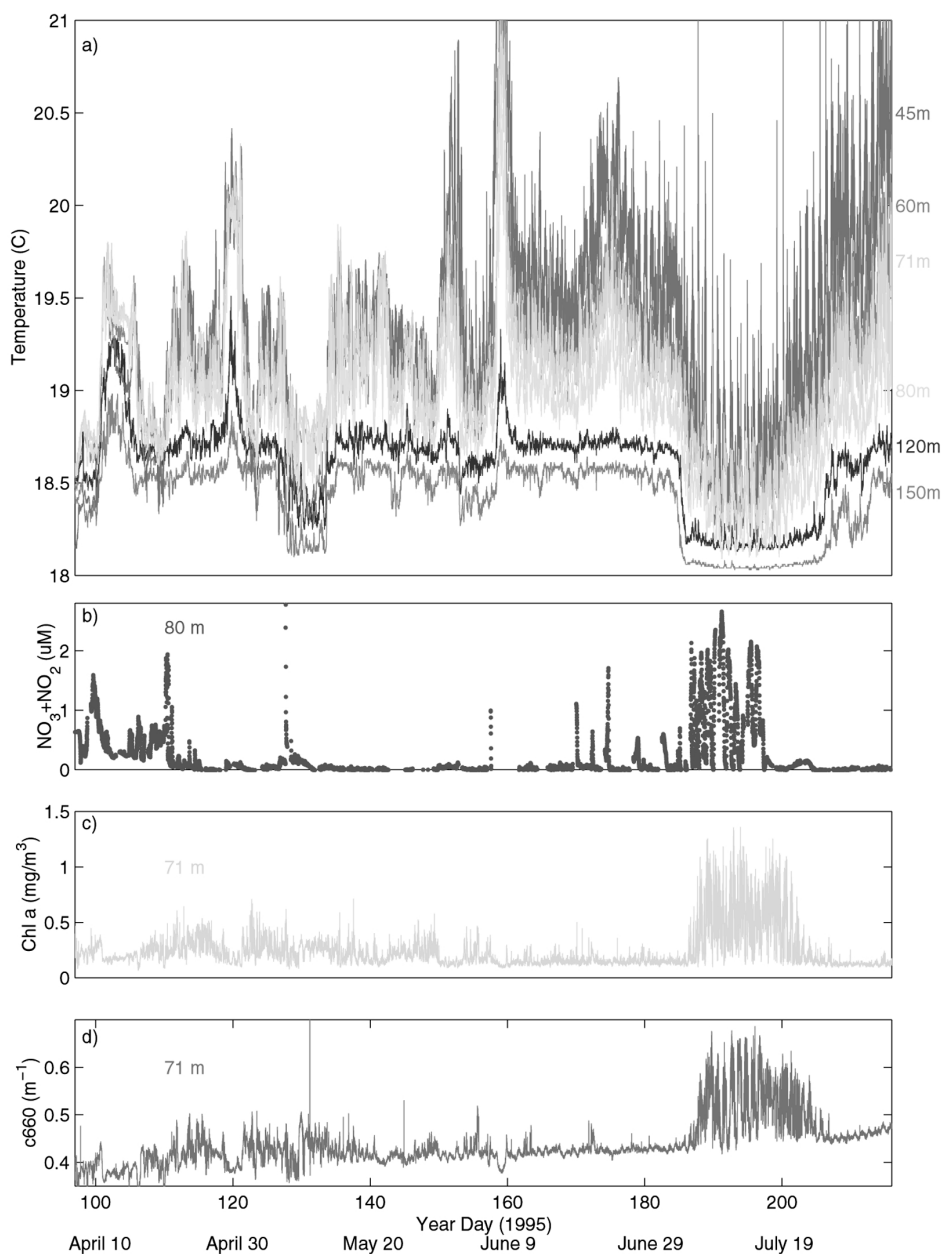
Fig. 10.7.   See color insert. Time series of data collected from the Bermuda Testbed Mooring in 1995. Variables are (*a*) temperature, (*b*) nitrate plus nitrite concentration, (*c*) chlorophyll *a*, and (*d*) beam *c*. Several nitrate "injections" are accompanied by bloom events. The passage of a major eddy is evident in July with decreased upper ocean temperature and large concentrations of nitrate + nitrite and chlorophyll *a*. (After McNeil et al., 1999.)

absorption of light was developed using high-temporal resolution data from the site in order to partition contributions by phytoplankton, detritus, and colored dissolved material (CDM) (Chang and Dickey, 1999). Besides the obvious effects of Hurricane Edouard and a later hurricane (Hortense), bloom conditions were also evident.

In the central Arabian Sea, the seasonal physical cycle associated with the northeast (NE) and southwest (SW) monsoons is correlated with bio-optical properties of the ocean (Dickey et al., 1998b). The seasonal physical forcing features two mixed layer deepening and shoaling cycles per year (Fig. 10.8). The NE monsoon is characterized by steady northeasterly winds of moderate intensity (about 6 m s^{-1}), surface cooling, and convection, whereas the SW monsoon features strong, persistent southwesterly winds with greater intensity (up to 15 m s^{-1}). The NE monsoon drives deeper mixed layers (about 110 m depth) than the SW monsoon (about 80 m depth) because of the convective forcing. A half-yearly cycle in chlorophyll a (Fig. 10.8) is an important feature with seasonal blooms occurring late in each monsoon season and into the respective intermonsoon periods; the depth-integrated chlorophyll a tracks the 1% light level. Again, the classical Sverdrup hypothesis appears to be supported [a more detailed interdisciplinary model of the NE monsoon is presented in Wiggert et al., (2000)]. Mesoscale eddies play roughly equal roles in the evolution of chlorophyll a at the observational site (Fig. 10.8). Other aspects of these time series are described below.

Finally, the physical dynamics of the equatorial Pacific have become increasingly well understood over the past decade in large part because of the measurements made from the Tropical Atmosphere Ocean (TAO) mooring array (e.g., McPhaden, 1995). However, understanding of biological and optical variability has been limited because few dedicated ship-based experiments could be performed in such a remote region. In particular, only a few biological observations of chlorophyll and primary productivity were made each year prior to 1988; these were our only bases for annual estimates of chlorophyll and primary production for the expansive Pacific equatorial waveguide (e.g., Cullen et al., 1992). However, bio-optical instruments were added to the TAO physical mooring at 0°, 140°W for an 18-month period in 1992 and 1993 (Foley et al., 1997). This sampling period was most fortuitous as the observations spanned both El Niño and "normal" phases. During the El Niño, the mixed layer, the thermocline, and a very weak equatorial undercurrent were very deep (at times in excess of 150 m) and Kelvin waves (about a 60-day period) propagated eastward past the site (with depressions of the thermocline). Although the light levels were high, relatively high concentrations of nutrients, including iron, were deep; consequently, measured chlorophyll a concentrations in the upper layer were low (less than 0.2 mg m^{-3}). However, as "normal conditions" returned, Kelvin waves ceased and the thermocline and a strong equatorial undercurrent shoaled allowing for the transport of nutrients into the euphotic layer. Importantly, westward-propagating tropical instability waves (TIWs with periods of about 20 days) also contributed to large vertical upwelling cycles. TIWs are easily seen in the meridional current records (also in ocean color images; see Yoder et al., 1994) and appear to be manifest in the chlorophyll a time series, with values doubling and at times tripling those observed during the El Niño period. Importantly, strong, although highly complex coupling is evident between the physical processes (El Niño, Kelvin waves, and TIWs) and the phytoplankton biomass and primary productivity (here roughly proportional to chlorophyll a) of the equatorial Pacific. It is worth noting that Barber et al. (1996) have suggested that the passages of the TIWs are analogous to a natural iron
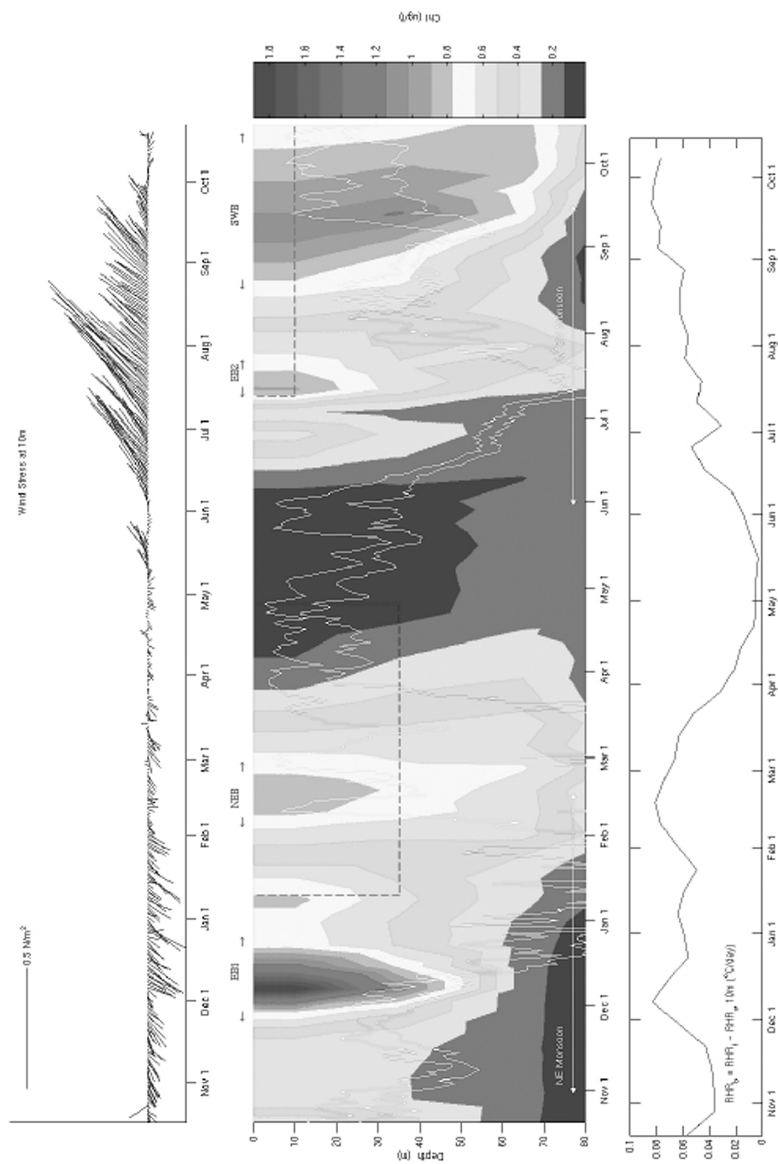
Fig. 10.8. See color insert. Top panel: Time series of wind stress vectors (winds "from" convention). Winds from the northeast, northeast monsoon, first appear in the record; these are followed by relatively calm winds (spring intermonsoon), and finally, the strong southwest monsoon winds. Middle panel: Time depth section of chlorophyll *a* concentration. Dashed boxes enclose periods and depths utilizing only shipboard data because of biofouling of moored fluorometers. Time series of mixed layer depth using 0.1°C criterion (shallower curve) and mixed layer depth using 1.0°C criterion (deeper curve). Time periods of eddy blooms, EB1 and EB2, and monsoonal blooms, NEB and SWB, are also indicated. Bottom panel: Time series (based on eight-day averages) of the biological radiant heating rate for the upper 10 m. (After Dickey et al., 1998b.)

enrichment experiment. The more recent 1997–1998 El Niño has also been documented using moored bio-optical instrumentation along with SeaWiFS ocean color satellite imagery data sets (Chavez et al., 1998, 1999).

4.2. *Biogeochemical Cycling: Biological Pump*

The reservoir of dissolved inorganic carbon (DIC) in the oceans is approximately 50-fold higher than the CO_2 in the atmosphere, and on geological time scales the oceans dictate the atmospheric concentration of the gas rather than vice versa. In the oceans there is an inverse gradient in dissolved inorganic carbon such that higher concentrations are found below the upper mixed layer, while to a first order, the upper portion of the water column is in equilibrium with the atmosphere. This inverse gradient is maintained by two carbon "pumps" (Volk and Hoffert, 1985). The solubility pump operates on the thermal contrast between the upper ocean and the ocean interior. The solubilities of cold waters of the deep ocean are on the order of twice as great as near-surface equatorial waters. Thus, the net effect of sinking of surface waters through thermohaline circulation is the enrichment of deeper waters in carbon. Superimposed on the solubility pump is a biological pump. In this process, phytoplankton living in the upper layer (euphotic layer) of the ocean use carbon dioxide to form organic matter. Much of the organic matter is metabolized; however, a significant portion (roughly 20%, but highly variable in terms of location and time) sinks to the deeper reaches of the ocean before being converted back to carbon dioxide (remineralization) by bacteria. Although currents later bring the carbon dioxide back to the surface, the overall effect is to transport carbon to the deep ocean. The solubility and biological pumps have significant impacts on atmospheric carbon dioxide levels (e.g., Sarmiento, 1993). The biological pump includes pathways of carbon to the deeper layers through dissolved organic carbon (DOC) molecules and particulate organic carbon (POC) matter.

There are several interesting connections between bio-optics, biogeochemistry, upper ocean physics, and the biological pump. As described earlier, primary productivity and phytoplankton biomass are dependent on photosynthetic processes, which implicitly involve the availability of light (e.g., PAR) and nutrients. Macronutrients (e.g., nitrate, silicate, and phosphate) and micronutrients (e.g., iron) are important. The spectral quality of light varies with depth and is important for specific phytoplankton species with special pigmentation or photoadaptive characteristics, as described earlier (e.g., see also Bidigare et al., 1990; Bissett et al., 1999). Light exposure for individuals is affected by variation in physical conditions, including mixed layer depth, turbulent mixing, and currents as well as incident solar radiation, which varies in time and space (e.g., astronomical forcing, cloud variability). An important feedback concerns the modulation of the spectral light field at depth as phytoplankton concentrations and communities wax and wane. The determination of primary production in the upper ocean is a vital step in quantifying the carbon flux associated with the biological pump (Laws et al., 2000). Fundamental measurements and models have been developed to estimate primary production [e.g., review by Behrenfeld and Falkowski (1997a) and Table I]. Such models often use measurements of chlorophyll *a* concentration and PAR. The choices of values for spectral absorption and quantum efficiency are often critical, as both of these parameters can vary in time and geographically.

Primary production has been estimated for a variety of geographic regions using remote sensing (Platt and Sathyendranath, 1991; Longhurst et al., 1995; Antoine et al., 1996; Behrenfeld and Falkowski, 1997b) as described earlier and from time series moorings (e.g., Dickey, 1991). For example, primary productivity, $P(z)$, has been estimated using some of the mooring data described earlier along with relatively simple models using $Chl(z)$ and $PAR(z)$ data. In some cases, best estimates or measurements of chlorophyll a, specific absorption coefficient for phytoplankton, a^*, and quantum yield for carbon fixation, $\Phi(z)$, have been utilized (e.g., Falkowski and Raven, 1997; Marra et al., 1999) in the following formulation:

$$P(z) = a^* \Phi(z) \, Chl(z) \, PAR(z) \tag{4}$$

Particular examples following this general methodology include the seasonal evolution of primary production in the North Atlantic (e.g., Marra et al., 1992), the ENSO and equatorial longwave effects on primary production in the equatorial Pacific (Foley et al., 1997), and the monsoonal cycle of primary production in the Arabian Sea (Marra et al., 1999). Again, one of the deficiencies of this method is that neither a^* nor Φ is constant because of community structure changes and varying light and nutrient stresses.

For some time there has been an implied connection between upper ocean primary production and export of carbon to the deep ocean; however, quantifying this relationship has been difficult because of the complexity of the processes, disparities in sampling methods and their resolutions, and lack of coincidence of upper ocean and deep-ocean measurements (e.g., Eppley and Peterson, 1979; Lewis, 1992; Platt et al., 1992). Recent collaborative work in the Arabian Sea using moored bio-optical and physical instrumentation (as described above; Dickey et al., 1998b) and deep moored sediment traps has apparently demonstrated that upper ocean primary productivity (Marra et al., 1998) is imprinted in deeper sediment records, which include exported organic and inorganic carbon (Honjo and Weller, 1999). The primary production time series was shown to vary in response to the two major effects described earlier: blooms associated with the northeast and southwest monsoons and the passage of major mesoscale eddies. The variability in the sediment trap carbon data correlated very well with the monsoonal cycle and eddy primary productivity events. These observations and estimates of primary productivity and phytoplankton biomass emphasize the need for high temporal and spatial resolution sampling because of the episodic and highly spatially variable nature of the physical, bio-optical, and biogeochemical processes contributing to the biological pump process.

4.3. Ultraviolet Radiation and Its Effect on Biological Processes

The flux of solar ultraviolet (UV) radiation reaching Earth's surface is critically dependent on the concentration of O_3 and, to a lesser extent, O_2 in the atmospheric column. Absorption bands between 190 and 350 nm are present in a wide variety of biological molecules. Interaction of UV radiation with such molecules can ionize quasistable (i.e., bonding) electrons. As water per se has a very small UV absorption cross section, UV entering the water column has a potential to interact with chromophores in the water column. Three of the most critical chromophores are the aromatic amino acids, quinones, and nucleic acids (Setlow, 1974). The first of these

are components of all proteins. The second is an electron transfer component in photosynthesis and respiration. The third is essential for cell division and protein synthesis. Action spectra for UV damage reveal two major targets: the photosynthetic apparatus and the nucleus. In the former, UV can exacerbate photoinhibition, apparently by damaging either the tyrosine donor to photosystem II and/or the quinone acceptor (Kok, 1956; Prasil et al., 1992). The damage to DNA occurs at several levels, but most importantly, leads to mutations in both the vegetative cells of plants or the somatic cells of animals. In both cases, protection and repair mechanisms have evolved to help reduce the damaging effects (Halldal and Taube, 1972; Cullen and Lesser, 1991; Cullen and Neale, 1993). Nonetheless, the flux of UV radiation can be markedly influenced by atmospheric changes in O_3 and can potentially lead to altered community structure of the plankton, especially at high latitudes (Karentz and Lutze, 1990; Smith et al., 1992). Given that UV fluxes have been a component of solar radiation since the formation of the Sun, it is reasonable to assume that the natural mutagenic and teratogenic effects of this weakly ionizing radiation have been both a selection mechanism and stimulus of biological diversity in the oceans for billions of years. In fact, bacteriochlorophylls do not directly absorb PAR but have strong UV absorption bands (Blankenship, 1992), and it has been suggested that these pigments actually were selected to screen against UV radiation in the Archean ocean (Mulkidjanian and Junge, 1996). The protection mechanisms involve the synthesis of benign UV-absorbing chromophores (nonprotein amino acids) that dissipate the radiation and simultaneously alter the UV absorption cross section in the water column (Dunlap and Chalker, 1986; Karentz, 1994).

4.4.   Radiant Heating Rate Modulation by Plankton

One of the clearest examples of biology affecting physical processes is the modulation of upper ocean heating rates by variability in phytoplankton and their associated pigment concentrations and related optical characteristics. Because phytoplankton absorb visible radiation in spectral regions that are relatively transparent for water itself, these photosynthetic organisms are potentially capable of altering the upper ocean heat budget. The extent to which this occurs depends on the concentration and vertical distribution of pigments within the water column, as well as the incident spectral irradiance. Intuitively, one can understand the effect by considering two bodies of water, lying side by side—swimming pools, for example. If one adds black ink to one pool while keeping the second clear, the darker pool will absorb virtually all of the incident solar radiation and become warmer faster. This effect is used to heat water in rooftop solar systems for homes. Similarly, the addition of phytoplankton to the upper ocean can have measurable effects on the rate of heating of the euphotic zone, with consequences for the depth of the upper mixed layer and vertical eddy diffusivity (e.g., Lewis et al., 1983, 1988).

Several modeling studies in the 1980s explored the sensitivity of upper ocean heating rates and ocean dynamics (e.g., heat content, currents, and mixing parameters) using various formulations and empirical values for the attenuation of solar radiation (e.g., Denman, 1973; Zaneveld and Spinrad, 1980; Simpson and Dickey, 1981a,b; Dickey and Simpson, 1983; Lewis et al., 1983, 1990; Woods et al., 1984; Woods and Barkmann, 1986; Lewis, 1987; Siegel and Dickey, 1987; Morel, 1988). The simplified one-dimensional heat budget equation (with no advection) for these studies can

be expressed as

$$\rho_0 c_p \frac{\partial T}{\partial t} = -\frac{\partial (E_n + J_q)}{\partial z} \tag{5}$$

where ρ_0 is the seawater density, c_p the specific heat constant of seawater, $T(z)$ the water column temperature, $E_n(z)$ the net $(E_d - E_u)$ irradiance (note that often the downward component is much greater than the upward component, or $E_d \gg E_u$; coccolithohphore blooms represent an important exception), J_q the vertical turbulent heat flux, and z the vertical coordinate (positive down).

The several studies cited above have demonstrated that physical mixed layer models should include proper parameterization of the penetrative component of solar radiation. Diurnal and seasonal heating cycles have been examined using various parameterizations (e.g., Dickey and Simpson, 1983; Woods et al., 1984). For the most part, the early model parameterizations were necessarily based on classical regional optical water types (e.g., Jerlov, 1976) because of the paucity of spectral optical measurements. A summary and model intercomparisons of several parameterizations of downward irradiance for clear ocean (type I) waters (Jerlov, 1976) is presented in Simpson and Dickey (1981b).

Importantly, the parameterizations were typically formulated as either empirical single or double exponential functions, with the latter representing the broad attenuation effects due to two separate wavebands (one for the red and infrared portion and one for the blue to green). Although limited subsurface spectral light data were available at the time of these studies, it is interesting to note that some exploration of the effects of finer spectral decomposition had begun (e.g., Simpson and Dickey, 1981b; Woods et al., 1984) with formulations of the general form

$$E_d(z) = \sum A_i \exp(-K_i z) \tag{6}$$

where the summation index i identifies the wavelength of a particular waveband, A_i a weighting factor for the particular waveband, and K_i the spectral diffuse attenuation coefficient for the corresponding waveband. Today's technology enables direct in situ measurements of E_d and E_u at multiple (commonly seven or more) wavelengths, typically with a bandwidth of about 10 nm. As a consequence, it is possible to apply spectral forms (e.g., like equation 6) to determine radiant heating rates and their temporal and spatial variability. It should be noted that even if such advanced measurements are not available, it is still preferable to utilize pigment (i.e., chlorophyll a) data and empirical models (e.g., Morel, 1988; Morel and Antoine, 1994) to estimate the spectral attenuation coefficient of light for mixed layer radiant heating rates (e.g., Dickey et al., 1998b). The empirical spectral dependence of the diffuse attenuation coefficient as a function of chlorophyll concentration (for wavelengths from 300 to 2400 nm) has been described by Morel and Antoine (1994, eq. 9). Given this brief introduction to the theoretical and practical issues of this problem, let us consider examples from a few diverse regional and global case studies.

The "spring bloom" phenomenon is a good example of large-scale physical–biological interactions. However, a more subtle aspect concerns the possibility of a positive feedback (as depicted in Fig. 10.2). For example, modest near-surface strat-

ification can contribute to a shallow phytoplankton bloom, which may be sufficient to cause increased local heating there and thus result in further increased stratification. This effect was observed when concurrent physical and bio-optical time series were collected in open ocean waters south of Iceland (59°29′N, 20°50′W; Dickey et al., 1994) in the spring of 1989. Remarkably, the mixed layer shoaled from about 550 m to about 50 m in only five days. Analysis of this data set suggested that incipient stratification was indeed enhanced by a phytoplankton bloom. This was supported by specific model simulations, which included the observed phytoplankton effect (Stramska and Dickey, 1993). In particular, it was shown that by including the biological effect, near-surface temperature was increased by about 0.2°C. Also, a shallower mixed layer, stronger stratification, and better agreement with observations resulted. Normally, transient winds and eddies affect the importance of near-surface biology for specific observations.

The equatorial Pacific has been the subject of intense study because of weather and climate implications; thus, heat budgets and fluxes have been central foci. The importance of the penetrative component of solar radiation in the region was first suggested by Lewis (1987). A simple heat flux scale analysis, based on a variety of data sets, was also done for this oceanic region by Siegel and Dickey (1987). Their work indicated that based on turbulence measurements and estimates of solar penetration, turbulent heat flux could equal radiant heat flux at depths of about 40 to 60 m for modest winds (<5 m s^{-1}). Other studies also argued for the inclusion of the penetrative component in analyses and models of the equatorial Pacific. For example, Lewis et al. (1990) noted that sea surface temperatures, which were being modeled using ship-based heat fluxes (and excluded the penetrative component of solar radiation), were overestimated in the western Pacific by up to 3°C. They used satellite water color transparency determinations, climatological surface heat fluxes, and density profiles to show that solar radiation often penetrates well below the mixed layer. The effect of this penetration was found to cause a reduction in heat input to the mixed layer, so that for a 20-m mixed layer, there would be a temperature reduction of about 5 to 10°C per year, bringing the heat budget much closer to balance. They also noted that an increase in phytoplankton concentration in the western equatorial Pacific to values more commonly observed in the eastern side (about 0.3 mg m^{-3}) would result in heat trapping of about 10 W m^{-2} in the upper ocean. Chlorophyll values of this magnitude occurred in the western Pacific during the 1982–1983 ENSO event. Direct measurements of bio-optical as well as physical variables have been made in the warm-water pool of the western Pacific (Siegel et al., 1995; Ohlmann et al., 1998). This work is supportive of the previous assertions concerning the importance of the penetrative component of solar radiation and more generally biogeochemical processes. For example, it was determined that common values of the penetrative solar flux are about 23 W m^{-2} at 30 m (the climatological mean mixed layer depth), and thus a large fraction of the climatological mean net air–sea flux of about 40 W m^{-2}. Synoptic scale forcing (e.g., wind bursts) were found to lead to tripling of phytoplankton pigment concentrations and a reduction in penetrative heat flux of 5.6 W m^{-2} at 30 m, or a biogeochemically mediated increase in the radiant heating rate of 0.13°C/month. In-depth analysis of the radiant heating and parameterizations of light attenuation for this experiment are given in Ohlmann et al. (1998). The equatorial Pacific is rich in biological variability, as emphasized by time series data described by Foley et al. (1997) and Chavez et al. (1998, 1999). As described above, these studies

have shown large variations in near-surface chlorophyll associated with El Niños, tropical instability waves, and Kelvin waves. Variability in biological radiant heating rates and solar penetration must necessarily be related as well. These collective results argue for continuous bio-optical measurements (e.g., irradiance, chlorophyll, and primary productivity) as part of physical mooring programs.

Annually, the Arabian Sea is forced by two major monsoonal episodes as shown in Fig. 10.8 and described earlier. Again, the northeast (NE) monsoon (November to February) is characterized by deep convection and moderate, steady wind forcing, whereas the southwest (SW) monsoon (June to September) is strongly wind driven (Weller et al., 1998). Thus, two mixed layer deepening events, as well as monsoonal phytoplankton blooms, occur each year. Sathyendranath et al. (1991) and Brock et al. (1993) conducted interdisciplinary modeling studies, which suggested the great importance of coupling of physics with phytoplankton variability, the subsurface light field, and biologically mediated upper ocean heating rates. In particular, Sathyendranath et al. (1991) predicted that biological heating rates could reach values of about 4°C month^{-1} at particular Arabian Sea locations. Field experiments were conducted in the Arabian Sea as part of the Joint Global Ocean Flux Study, with focus on biogeochemical cycling (e.g., Smith et al., 1998). As part of these experiments, radiant heating as affected by phytoplankton (chlorophyll) variability was estimated by Dickey et al. (1998b) using interdisciplinary mooring-based time series data and a modified form (depth dependence implemented) of a hybrid subsurface light field parameterization (Ohlmann et al., 1996) for an open ocean site (15°30′N, 61°30′E). They found strong modulation of the chlorophyll concentrations not only by the monsoonal forcing but also by mesoscale eddies, which were ubiquitous in the region. The biological heating rates reached values of about 2.5°C month^{-1} for the open ocean site (Fig. 10.8). It should be noted that radiant heating rates as well as the net penetrative heat flux estimates are dependent on the mixed layer depth criterion, so comparisons must be done with care. During the spring intermonsoon, the penetrative component reached values of about two-thirds of the surface net heat flux using a mixed layer depth (MLD) criterion of 0.1°C (0.1°C temperature difference between surface and defined mixed layer depth) and about one-third of the surface net heat flux using a 1°C MLD criterion (Dickey et al., 1998b). Clearly, omission of the penetrative component would lead to a significant biased error in the heat budget.

One of the more interesting phytoplankton groups is the coccolithophorids (see Figure 10.9). These organisms secrete external calcium carbonate plates or coccoliths (see Ackleson et al., 1988, 1994; Balch et al., 1991, 1996a,b) that strongly scatter light. Coccolithophorids evolved in the late Triassic period. By the Cretaceous, their blooms were so large and extensive that the geological deposition of calcium carbonate created by their calcifying activity was responsible for the vast deposition of chalk beds and limestones from the Mesozoic. At high concentrations, coccolithophores and coccoliths, which are highly reflective, cause ocean waters to appear milky white. These phytoplankton are relatively widespread (Holligan et al., 1993; Brown and Yoder, 1994) and at times dominate other phytoplankton groups, especially at high latitudes (Fig. 10.5). Coccolithophores are important because of (1) their effect on seawater chemistry (i.e., alkalinity and ΣCO_2); coccolithophores are capable of fixing carbon and increasing the level of $p CO_2$ in the surface layer; (2) their roles in biogeochemical cycling (e.g., calcification rates of coccolithophores affect carbon dioxide fluxes between the ocean and atmosphere and sinking of coccoliths
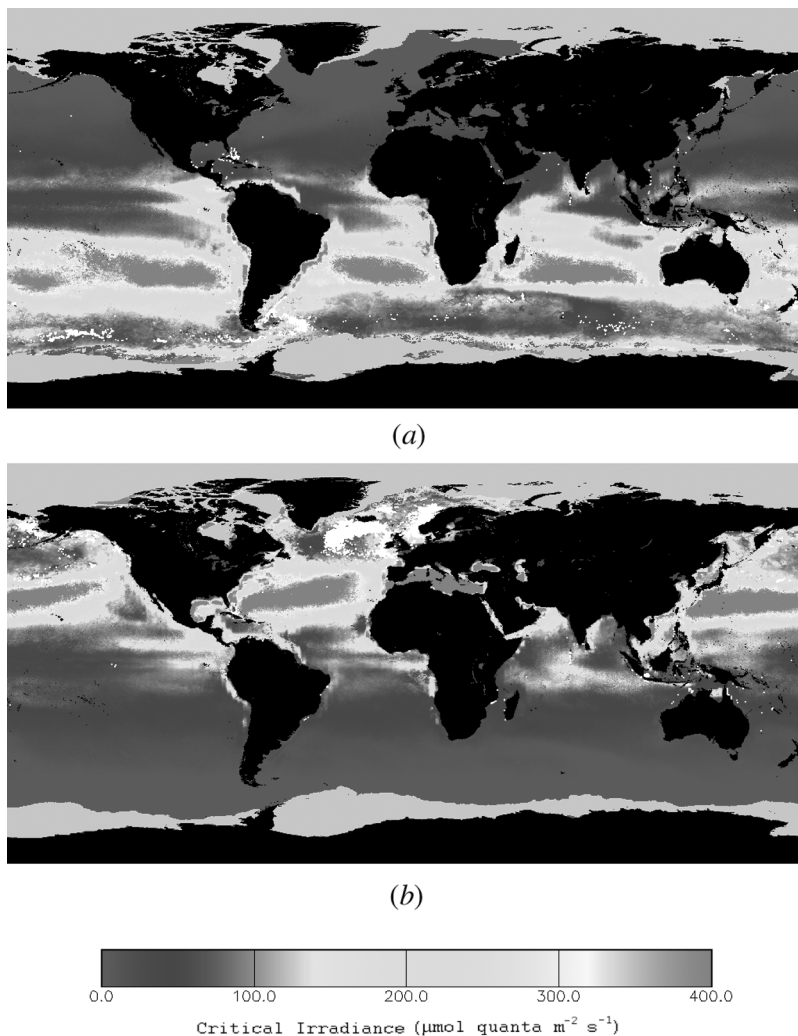
(*a*)

(*b*)

Critical Irradiance (μmol quanta m^{-2} s^{-1})

Fig. 10.9.   See color insert. (*a*) Winter and (*b*) summer distributions of coccolithophorids in the global ocean in relation to critical irradiance. The coccolithophorids are seen by satellite imagery as highly reflective pixels and are shown in the figures as white dots. Note their circumpolar distributions north of the Antarctic in the winter (austral summer) in panel *a* and the widespread distribution in the Northern Hemisphere in the summer in panel *b*. The critical irradiance is a measure of the total daily irradiance in the upper mixed layer.

takes carbon to the deep sea); (3) their effects on climate [release of dimethylsul-fide (DMS) as coccolithophores act as a major source of cloud condensation nuclei over the oceans]; (4) their impact on radiant heating effects; and (5) their local dom-inance of remotely sensed color imagery. Interestingly, Balch et al. (1991) noted that chemical changes often parallel optical changes (e.g., alkalinity and coccolithophore blooms shown to be inversely related to optical scattering of detached coccoliths) and Holligan et al. (1993) have reported positive correlations between beam attenuation and pCO$_2$.

Here we focus on the radiant heating aspect. Because coccolithophorids and their coccoliths are such strong scatterers (e.g., Bricaud and Morel, 1986), their role in radiative transfer of energy and their in situ optical characterization are far more difficult to model than for most other phytoplankton groups. Further, instrumentation for in situ spectral absorption measurements (e.g., Moore et al., 1992; Bruce et al., 1996) has become available only over the past few years, and only recently has spectral backscatter instrumentation been developed (e.g., Dana et al., 1998). Nonetheless, some important field studies of the biological and optical properties of coccolithophore blooms have provided new insights. For example, Balch et al. (1991) reported results of two field campaigns focusing on coccolithophore (*Emiliania huxleyi*) blooms in the Gulf of Maine. They found that about 80% of backscattered light at 550 nm was due to coccoliths and that near-surface reflectance ($R = E_u/E_d$) values ranged from over 0.2 to 0.3 for nonbloom waters of roughly similar chlorophyll concentrations; coccolith backscattering usually accounts for 10 to 20% of the total backscattering, with irradiance reflectance values of only a few percent (see also Balch et al., 1996a,b). Multiple scattering of light is clearly occurring during such blooms (and especially their remnant phases). Thus, radiative transfer theories, which impose single scattering assumptions, break down for coccolithophore blooms. Additionally, the longer effective pathlengths of light cause increases of light absorption in the near-surface waters allowing less light to penetrate to depth. This is supported by analysis of the same Gulf of Maine data by Ackleson et al. (1988), who reported that heating rates within one of the coccolithophore blooms were about 0.32°C day^{-1} compared with values of 0.06°C day^{-1} outside the bloom region. Satellite-derived surface temperature data indicated warmer water (by about 5°C) within the bloom area compared with adjacent outside waters. Solution of the coccolithophore heating problem will require both new in situ and remote sensing observations and the application of multiple-scattering radiative transfer models (e.g., Tyrell et al., 1999); however, use of presently available in situ spectral irradiance instrumentation can be very useful as well.

Global variability in water transparency and its potential effects on heat budgets and heating rates have been the subject of a few studies (e.g., Simonot and LeTreut, 1986; Lewis et al., 1988; Ohlmann et al., 1998). For example, Lewis et al. (1988) presented an analysis of climatological Secchi depth measurements (about 120,000 observations). While Secchi depth (roughly the depth of disappearance of a profiled 0.25-m white disk; a broadband visible light penetration depth) data provide rather imprecise information on water clarity, they have been collected as standard optical observations for several decades over many parts of the world ocean and provide our best view of optical climatology. Lewis et al. (1988) used an empirical formula to translate Secchi depth data into estimates of chlorophyll concentration. Interestingly, the inferred concentrations were in good agreement with the Coastal Zone Color Scanner (CZCS) satellite-based estimates and showed a major optical front traversing the ocean basins at about 10 to 30° N. Following this work, Falkowski and Wilson (1992) used a 90-year record of Secchi depth observations to examine whether phytoplankton biomass in the North Pacific Ocean had changed markedly in the twentieth century. Their results suggest that a small systematic increase in phytoplankton has occurred on the edges of the central ocean gyres, while the gyre core has undergone a small depletion of phytoplankton. One possible cause of these changes is enhanced gyre rotation due to higher wind speeds at the continental boundaries

(Bakun, 1990). Recent time series work in the central North Pacific (Karl, 1999) indicates that chlorophyll *a* concentrations and primary production in the surface waters there have more than doubled during the past three decades. The various studies using Secchi data can provide at least rough indications of longer-term variability and climatological trends in radiant heating rates. Finally, Ohlmann et al. (1998) have presented a regional/global analysis of mixed layer radiant heating and solar penetration. Input data included incident solar flux from the International Satellite Cloud Climatology Project and upper ocean chlorophyll concentration from CZCS. Some of the key results of the Ohlmann et al. (1998) analysis include: (1) solar penetration can be a significant fraction of the upper ocean mixed layer heat budget in the tropics and is important seasonally at mid- to high latitudes, and (2) annual climatological values of solar penetration can reach 40 W m^{-2}; omission would lead to overestimates of mixed layer heating of about 0.3°C month^{-1}.

5.   Enabling Methodologies: Theories and Technologies

Theories and models, which can be used to estimate IOPs from AOPs and vice versa, are being developed, but further advances are still needed. The theoretical framework for biological modulation of radiant heating rates is quite well developed for conditions where the single-scattering approximation is valid. However, media where multiple scattering is very important, such as areas where coccolithophore blooms are occurring or have recently occurred, are considerably more challenging and more theoretical work will be required (Tyrell et al., 1999).

Considerable progress has been made in expanding the number of bio-optical observations, which can be made on virtually the same time and space scales as physical measurements such as temperature, salinity, and currents. This is due in large part to development of new in situ sensors, many of which are fairly small, require low power, and have high spectral resolution. It is anticipated that the trend in this direction will continue and that as more sensors and systems are sold commercially, the cost will decrease. Measurements of spectral absorption, scattering, and attenuation coefficients are advancing rapidly with improved spectral resolution capability (Moore et al., 1992; Bruce et al., 1996; Dana et al., 1998).

Higher spectral resolution measurements are now available for irradiance and radiance (M. Lewis, personal communication). Spectral fluorescence measurements, which can be used for identifying dissolved materials have been developed as well (e.g., Desiderio et al., 1997; Petrenko et al., 1998). Key optical measurements are now being developed for volume scattering and backscattering (Dana et al., 1998). These measurements are important for several optical studies, especially for remote sensing (which relies on a small backscattering signal and is affected by whitecapping and bubbles) and when scattering represents a large portion of the optical attenuation (e.g., the coccolithophore/coccolith problem). These latter measurements are also necessary for developing models, which can be used for estimating IOPs from AOPs and the inverse problem.

The interpretation of optical and bio-optical measurements remains an important problem in large part due to the complexity of the measured bulk properties. In some cases, in situ "groundtruthing" has proven valuable (e.g., comparisons of ^{14}C primary production measurements with mooring-based estimates), but in others the collection of water samples for comparison with in situ measurements has proven problematic.

An interesting example concerns the interpretation of beam c(660 nm) data in terms of suspended particulate matter (SPM), particulate organic carbon (POC), and primary productivity (e.g., Siegel et al., 1989). Bishop (1999) conducted a series of experiments to ascertain relations between beam c(660 nm) and SPM and POC. He determined that considerably more robust relations (r^2 of 0.9 and greater) existed between beam c(660 nm) and POC than between beam c(660 nm) and SPM. This result is quite surprising considering the large number of interpretive complications described in Section 4.1. Nonetheless, the potential use of beam c to estimate POC is important, as POC is of direct importance for the carbon cycling and flux problem.

Commercial development of sensitive kinetic fluorometers capable of deriving photosynthetic rates and parameters in real time has dramatically altered our ability to understand how photobiological processes interact with physical processes. Such instrumentation can be adapted to a wide suite of oceanographic issues, such as nutrient limitation, photoinhibition of photosynthesis, species selection, and in situ primary production. Such instrumentation, based on the fast-repetition-rate fluorescence technique (Kolber et al., 1998), has been used to follow changes in photosynthetic solar energy conversion efficiency as a function of advection (Kolber et al., 1990), and nutrient stress (Falkowski, 1992).

Presently, most bio-optical sensors are deployed from ship-based profilers and to a lesser extent from moorings. With advances in microprocessor technologies, data processing and storage are not generally limiting. The need to expand the spatial and temporal ranges and resolutions of multidisciplinary in situ observations will require utilization of more autonomous platforms such as moorings, drifters, floats, gliders, and autonomous underwater vehicles (AUVs). Capabilities of all of these platforms are improving rapidly and their costs are decreasing. Remote sensing of ocean color is also advancing, with more satellites with higher spectral and spatial resolution (e.g., Davis et al., 1999; IOCCG, 1999). Near real-time data telemetry of optical and physical data is important for many applications. Telemetry technologies are improving rapidly with new communication systems, which can be either satellite or land-based (Dickey et al., 1993b). With increased numbers of low-earth-orbit (LEO) communication satellites, we can expect increased bandwidth and more frequent data transmissions.

Many of our examples have illustrated the complexity of the ocean ecosystem, including examples of the patchy and episodic nature of phytoplankton and bio-optical properties. The applications of moored fluorometers and other optical sensors represent the biological and optical equivalents of current meters, allowing high-frequency, long-time series of chlorophyll fluorescence and light properties to be obtained from multiple locations. These data suggest that phytoplankton distributions in the ocean are not "chaotic" in a mathematical sense but are also not easily predicted (Ascioti et al., 1993). There is clearly a great need for careful work to analyze and interpret the burgeoning optical data sets. A challenge for the future will be to understand and formulate the mathematical rules by which solar radiation and biological processes are coupled through physical forcing in the ocean.

On longer temporal and spatial scales, it is critical to examine whether Earth is a unique terrestrial planet or whether other planets in neighboring solar systems have liquid water on their surface. As life on this planet has been related directly to solar energy and its major electron source (water), so must we question whether our energy sources and sinks have been replicated elsewhere. This problem, namely how solar

energy interacts with biota in the oceans, is one of the most profound issues in science, one that relates every bit as much to how we interpret the future of our planet. If we consider that there are 10^{11} stars in our galaxy, and, based on the present rate of planet discovery in other solar systems, we can estimate that between 1 and 10% of the stars on our galaxy have one or more orbiting planets. Assuming that the accretion phenomenon that gave rise to our planetary system also gave rise to at least some other planetary systems (i.e., that inner planets are lithospheric and the outer planets have less dense cores), and assuming, purely on statistical grounds, that 1% of those planets is within a zone of habitability, we can conservatively estimate that there are between 10^6 and 10^7 planets capable of maintaining a film of liquid water on their surfaces. That is a large number indeed, and the knowledge of biological and optical oceanographers can contribute to their discovery.

Acknowledgments

References

Abbott, M. R., P. J. Richerson and T. M. Powell, 1982. In situ response of phytoplankton fluorescence to rapid variations in light. *Limnol. Oceanogr.*, **27,** 218–225.

Ackleson, S. G., W. M. Balch and P. M. Holligan, 1988. White waters of the Gulf of Maine. *Oceanography*, **1**(2), 18–22.

Ackleson, S. G., W. M. Balch and P. M. Holligan, 1994. The response of water-leaving radiance to particulate calcite and pigment concentration: a model for Guld of Maine coccolithophore blooms. *J. Geophys. Res.*, **99,** 7483–7499.

Antoine, D., J. M. Andre, et al., 1996. Oceanic primary production 2. Estimation at global-scale from satellite (coastal zone color scanner) chlorophyll. *Global Biogeochem. Cycles*, **10,** 57–69.

Arrigo, K. R. and C. W. Brown, 1996. Impact of chromophoric dissolved organic matter on UV inhibition of primary productivity in the sea. *Mar. Ecol. Prog. Ser.*, **140,** 207–216.

Ascioti, F. A., E. Beltrami, T. O. Carrol and C. Wirick, 1993. Is there chaos in plankton dynamics? *J. Plankton Res.*, **15,** 603–617.

Bakun, A., 1990. Global climate change and intensification of coastal ocean upwelling. *Science*, **247,** 198–201.

Balch, W. M., P. M. Holligan, S. G. Ackleson and K. J. Voss, 1991. Biological and optical properties of mesoscale coccolithophore blooms in the Gulf of Maine. *Limnol. Oceanogr.*, **36,** 629–643.

Balch, W. M., K. A. Kilpatrick, P. M. Holligan and C. C. Trees, 1996a. The 1991 coccolithophore bloom in the central North Atlantic. 1. Optical properties and factors affecting their distribution. *Limnol. Oceanogr.*, **41,** 1669–1683.

Balch, W. M., K. A. Kilpatrick, P. Holligan, D. Harbour and E. Fernandez, 1996b. The 1991 coccolithophore bloom in the central North Atlantic. 2. Relating optics to coccolith concentration. *Limnol. Oceanogr.*, **41,** 1684–1696.

Barber, R. T., M. P. Sanderson, S. T. Lindley, F. Chai, J. Newton, C. C. Trees, D. G. Foley and F. P. Chavez, 1996. Primary productivity and its regulation in the equatorial Pacific during and following the 1991–1992 El Niño. *Deep-Sea Res. II*, **43,** 933–970.

Behrenfeld, M. and P. G. Falkowski, 1997a. A consumer's guide to phytoplankton primary productivity models. *Limnol. Oceanogr.*, **42,** 1–20.

Behrenfeld, M. and P. G. Falkowski, 1997b. Phytosynthetic rates derived from satellite-based chlorophyll concentration. *Limnol. Oceanogr.*, **42,** 1479–1491.

Bidigare, R. R., J. Marra, T. D. Dickey, R. Iturriaga, K. S. Baker, R. C. Smith and H. Pak, 1990. Evidence for phytoplankton succession and chromatic adaptation in the Sargasso Sea during springtime 1985. *Mar. Ecol. Progr. Ser.*, **60,** 113–122.

Bishop, J. K. B., 1999. Transmissometer measurement of POC. *Deep-Sea Res. I*, **46,** 353–369.

Bissett, W. P., J. J. Walsh, D. A. Dieterle and K. L. Carder, 1999. Carbon cycling in the upper waters of the Sargasso Sea. I. Numerical simulation of differential carbon and nitrogen fluxes. *Deep-Sea Res. I*, **46,** 205–269.

Blankenship, R. E., 1992. Origin and early evolution of photosynthesis. *Photosyn. Res.*, **33,** 91–111.

Bothwell, M. L., D. M. J. Sherbot and C. M. Pollock, 1994. Ecosystem response to solar ultraviolet-b radiation: influence of trophic-level interactions. *Science*, **265,** 97–100.

Bricaud, A. and A. Morel, 1986. Light attenuation and scattering by phytoplankton cells: a theoretical model. *Appl. Opt.*, **25,** 571–580.

Brock, J., S. Sathyendranath and T. Platt, 1993. Modeling the seasonality of subsurface light and primary production in the Arabian Sea. *Mar. Ecol. Prog. Ser.*, **101,** 209–221.

Brown, C. W. and J. A. Yoder, 1994. Coccolithophorid blooms in the global ocean. *J. Geophys. Res.*, **99,** 7467–7482.

Bruce, E. J., M. Morgerson, C. Moore and A. Weidemann, 1996. Hi-Star: a spectrophotometer for measuring the absorption and attenuation of waters in situ and in the laboratory. *Ocean Optics XIII, SPIE*, **2963,** 637–642.

Buiteveld, H., J. H. M. Hakvoort and M. Donze, 1994. Optical properties of pure water. *Ocean Optics XII, SPIE*, **2258,** 174–183.

Butler, W. L., 1972. On the primary nature of fluorescence yield changes associated with photosynthesis. *Proc. Natl. Acad. Sci. USA*, **69,** 3420–3422.

Carder, K. L. and R. G. Steward, 1985. A remote-sensing reflectance model of a red-tide dinoflagellate off west Florida. *Limnol. Oceanogr.*, **30,** 286–298.

Carpenter, E. J., B. Bergman, R. Dawson, P. J. A. Siddiqui, E. Soederbaeck and D. G. Capone, 1992. Glutamine synthetase and nitrogen cycling in colonies of the marine diazotrophic cyanobacteria *Trichodesmium* spp. *Appl. Environ. Microbiol.*, **58,** 3122–3129.

Chang, G. C. and T. D. Dickey, 1999. Partitioning in situ total spectral absorption by use of moored spectral absorption and attenuation meters. *Appl. Opt.*, **38,** 3876–3887.

Chang, G. C. and T. D. Dickey, 2001. Optical and physical variability on time scales from minutes to the seasonal cycle on the New England continental shelf: July 1996–June 1997. *J. Geophys. Res.*, **106,** 9435–9453.

Chavez, F., P. G. Strutton and M. J. McPhaden, 1998. Biological–physical coupling in the central Pacific during the onset of the 1997–98 El Niño. *Geophys. Res. Lett.*, **25,** 3543–3546.

Chavez, F. P., P. G. Strutton, G. E. Friederich, R. A. Feely, G. C. Feldman, D. G. Foley and M. J. McPhaden, 1999. Biological and chemical response of the equatorial Pacific Ocean to the 1997–98 El Niño. *Science*, **286,** 2126–2131.

Chisholm, S. W., F. M. Morel and W. S. Slocum, 1980. The phasing and distribution of cell division cycles in marine diatoms. In *Primary Productivity in the Sea*, P. G. Falkowski, ed. Plenum Press, New York, pp. 281–300.

Crowley, T. and G. North, 1991. *Paleoclimatology*. Oxford University Press, New York.

Cuhel, R. L., P. B. Ortner and D. R. S. Lean, 1984. Night synthesis of protein by algae. *Limnol. Oceanogr.*, **29,** 731–744.

Cullen, J. J., 1982. The deep chlorophyll maximum: comparing vertical profiles of chlorophyll *a. Can. J. Fish. Aquat. Sci.*, **39,** 791–803.

Cullen, J. J. and M. P. Lesser, 1991. Inhibition of photosynthesis by ultraviolet radiation as a function of dose and dosage rate: results for a marine diatom. *Mar. Biol.*, **111,** 183–190.

Cullen, J. J. and M. R. Lewis, 1995. Biological processes and optical measurements near the sea-surface: some issues relevant to remote sensing. *J. Geophys. Res.*, **100,** 13255–13266.

Cullen, J. J. and P. J. Neale, 1993. Ultraviolet radiation, ozone depletion, and marine photosynthesis. *Photosyn. Res.*, **39,** 303–320.

Cullen, J. J., M. R. Lewis, C. O. Davis and R. T. Barber, 1992. Photosynthetic characteristics and estimated growth rates indicate grazing is the proximate control of primary production in the equatorial Pacific. *J. Geophys. Res.*, **97,** 639–654.

Cullen, J. J., A. M. Ciotti, R. F. Davis and M. R. Lewis, 1997. Optical detection and assessment of algal blooms. *Limnol. Oceanogr.*, **42,** 1223–1239.

Dana, D. R., R. A. Maffione and P. E. Coenen, 1998. A new in situ instrument for measuring the backward scattering and absorption coefficients simultaneously, *Ocean Optics XIV*, **1,** 1–8.

Davis, C. O., 1997. The Hyperspectral Remote Sensing Technology (HRST) program. In *Proceedings of the ASPRS Meeting: Land Satellite Information in the Next Decade. II. Sources and Applications*, December 2–5, Washington, D.C.

Davis, C. O., M. Kappus, B.-C. Gao, W. P. Bissett and W. Snyder, 1999. The Naval Earth Map Observer (NEMO) science and naval products. *SPIE*, **3437.**

de Mora, S., S. Demers and M. Vernet, 2000. *The Effects of UV Radiation on the Marine Environment*. Cambridge Environmental Chemistry Series. Cambridge University Press, Cambridge.

Denman, K. L., 1973. A time-dependent model of the upper ocean. *J. Phys. Oceanogr.*, **3,** 173–184.

Desiderio, R. A., C. Moore, C. Lantz and T. J. Cowles, 1997. Multiple excitation fluorometer for in situ oceanographic applications. *Appl. Opt.*, **36,** 1289–1296.

Dickey, T., 1991. Concurrent high resolution physical and bio-optical measurements in the upper ocean and their applications. *Rev. Geophys.*, **29,** 383–413.

Dickey, T. D. and J. J. Simpson, 1983. The influence of optical water type on the diurnal response of the upper ocean. *Tellus*, **35,** 142–151.

Dickey, T., J. Marra, T. Granata, C. Langdon, M. Hamilton, J. Wiggert, D. Siegel and A. Bratkovich, 1991. Concurrent high resolution bio-optical and physical time series observations in the Sargasso Sea during the spring of 1987. *J. Geophys. Res.*, **96,** 8643–8663.

Dickey, T., T. Granata, J. Marra, C. Langdon, J. Wiggert, Z. Chai-Jochner, M. Hamilton, J. Vazquez, M. Stramska, R. Bidigare and D. Siegel, 1993a. Seasonal variability of bio-optical and physical properties in the Sargasso Sea. *J. Geophys. Res.*, **98,** 865–898.

Dickey, T. D., R. H. Douglass, D. Manov, D. Bogucki, P. C. Walker and P. Petrelis, 1993b. An experiment in duplex communication with a multi-variable moored system in coastal waters. *J. Atmos. Ocean. Technol.*, **10,** 637–644.

Dickey, T., J. Marra, M. Stramska, C. Langdon, T. Granata, R. Weller, A. Plueddemann and J. Yoder, 1994. Bio-optical and physical variability in the sub-arctic North Atlantic Ocean during the spring of 1989. *J. Geophys. Res.*, **99,** 22541–22551.

Dickey, T., D. Frye, H. Jannasch, E. Boyle, D. Manov, D. Sigurdson, J. McNeil, M. Stramska, A. Michaels, N. Nelson, D. Siegel, G. Chang, J. Wu and A. Knap, 1998a. Initial results from the Bermuda Testbed Mooring Program. *Deep-Sea Res. I*, **45,** 771–794.

Dickey, T., J. Marra, R. Weller, D. Sigurdson, C. Langdon and C. Kinkade, 1998b. Time-series of bio-optical and physical properties in the Arabian Sea: October 1994–October 1995. *Deep-Sea Res. II*, **45,** 2001–2025.

Dickey, T., D. Frye, J. McNeil, D. Manov, N. Nelson, D. Sigurdson, H. Jannasch, D. Siegel, A. Michaels and R. Johnson, 1998c. Upper ocean temperature response to hurricane Felix as measured by the Bermuda Testbed Mooring. *Mon. Weather Rev.*, **126,** 1195–1201.

Dickey, T. D., G. C. Chang, Y. C. Agrawal, A. J. Williams 3rd and P. S. Hill, 1998d. Sediment resuspension in the wakes of hurricanes Edouard and Hortense. *Geophys. Res. Lett.*, **25,** 3533–3536.

Dunlap, W. C. and B. E. Chalker, 1986. Identification and quantitation of near-UV absorbing compounds (S-320) in a hermatypic scleractinian. *Coral Reefs*, **5,** 155–159.

DuRand, M. D. and R. J. Olson, 1996. Contributions of phytoplankton light scattering and cell concentration changes to diel variations in beam attenuation in the equatorial Pacific from flow cytometric measurements of pico-, ultra-, and nanoplankton. *Deep-Sea Res. II*, **43,** 891–906.

Duysens, L. N. M., 1956. The flattening of the absorption of suspensions, as compared to that of solutions. *Biochim. Biophys. Acta*, **19,** 1–12.

Einstein, A., 1910. Theorie der Opaleszenz von homogenen Flüssigkeiten un Flüssigkeitsgemischen in der Nähe des kritischen Zustandes. *Ann. Phys.*, **33,** 1275.

Eppley, R. W. and B. J. Peterson, 1979. Particulate organic matter flux and planktonic new production in the deep ocean. *Nature*, **282,** 677–680.

Escoubas, J.-M., M. Lomas, et al., 1995. Light intensity regulation of cab gene transcription is signaled by the redox state of the plastoquinone pool. *Proc. Nat. Acad. Sci. USA*, **92,** 10237–10241.

Falkowski, P. G., 1983. Light–shade adaptation and vertical mixing of marine phytoplankton: a comparative field study. *J. Mar. Res.*, **41,** 215–237.

Falkowski, P. G., 1984. Physiological responses of phytoplankton to natural light regimes. *J. Plankton Res.*, **6,** 295–307.

Falkowski, P. G., 1992. Molecular ecology of phytoplankton photosynthesis. In *Primary Productivity and Biogeochemical Cycles in the Sea*, P. G. Falkowski, ed. Plenum Press, New York, pp. 47–67.

Falkowski, P., 1997. Evolution of the nitrogen cycle and its influence on the biological sequestration of CO_2 in the ocean. *Nature*, **387,** 272–275.

Falkowski, P. G. and Z. Kolber, 1995. Variations in chlorophyll fluorescence yields in phytoplankton in the world oceans. *Aust. J. Plant Physiol.*, **22,** 341–355.

Falkowski, P. G. and J. A. Raven, 1997. *Aquatic Photosynthesis*. Blackwell Scientific Publishers, Oxford.

Falkowski, P. G. and C. Wilson, 1992. Phytoplankton productivity in the North Pacific ocean since 1900 and implications for absorption of anthropogenic CO_2. *Nature*, **358,** 741–743.

Falkowski, P. G., D. Ziemann, Z. Kolber and P. K. Bienfang, 1991. Role of eddy pumping in enhancing primary production in the ocean. *Nature*, **352,** 55–58.

Falkowski, P. G., R. Greene and R. Geider, 1992. Physiological limitations on phytoplankton productivity in the ocean. *Oceanography*, **5**(2), 84–91.

Foley, D., T. Dickey, M. McPhaden, R. Bidigare, M. Lewis, R. Barber, C. Garside and D. Manov, 1997. Longwaves and primary productivity variations in the equatorial Pacific at 0°, 140° W. *Deep-Sea Res. II*, **44,** 1801–1826.

Forward, R., Jr., 1988. Diel vertical migration: zooplankton photobiology and behavior. *Oceanogr. Mar. Biol. Annu. Rev.*, **26,** 361–392.

Gardner, W. D., S. P. Chung, M. J. Richardson and I. D. Walsh, 1995. The oceanic mixed layer pump. *Deep-Sea Res. II*, **42,** 757–775.

Garver, S. A. and D. A. Siegel, 1998. Inherent optical property inversion of ocean color spectra and its biogeochemical interpretation. 1. Time series from the Sargasso Sea. *J. Geophys. Res.*, **102,** 18607–18625.

Gieskes, W. C. and A. G. J. Buma, 1997. UV damage to plant life in a photobiologically dynamic environment: the case of marine phytoplankton. *Plant Ecol.*, **128,** 16–25.

Gordon, H. R., 1994. Modeling and simulating radiative transfer in the oceans. In *Ocean Optics*, R. W. Spinrad, K. L. Carder and M. J. Perry, eds. Oxford University Press, Oxford.

Gordon, H. R., O. B. Brown and M. M. Jacobs, 1975. Computed relationships between the inherent and apparent optical properties of a flat homogeneous ocean. *Appl. Opt.*, **14,** 417–427.

Gordon, H. R., O. B. Brown, R. H. Evans, J. W. Brown, R. C. Smith, K. S. Baker and D. K. Clark. 1988. A semianalytic radiance model of ocean color. *J. Geophys. Res.*, **93,** 10909–10924.

Gran, H. H., 1931. On the conditions for the production of plankton in the sea. *Rapp. P.-V. Reun. Cons. Int. Explor. Mer.*, **75,** 37–46.

Granata, T., J. Wiggert and T. Dickey, 1995. Trapped, near inertial waves and enhanced chlorophyll distributions. *J. Geophys. Res.*, **100,** 20793–20804.

Halldal, P. and O. Taube, 1972. Ultraviolet action spectra and photoreactivation in algae. *Photophysiol.*, **6,** 445–460.

Hamilton, M., T. C. Granata, T. D. Dickey, J. D. Wiggert, D. A. Siegel, J. Marra and C. Langdon, 1990. Diel variations of bio-optical properties in the Sargasso Sea. *Ocean Optics X*, pp. 214–224.

Hayward, T. L. and E. L. Venrick, 1982. Relation between surface chlorophyll, integrated chlorophyll and integrated primary production. *Mar. Biol.*, **69,** 247–252.

Holligan, P. M., E. Fernandez, J. Aiken, W. M. Balch, P. Boyd, P. H. Burkhill, M. Finch, S. B. Groom, G. Malin, K. Muller, D. Purdie, C. Robinson, C. C. Trees, S. M. Turner and P. van der Wal, 1993. A biogeochemical study of coccolithophore *Emiliania huxleyi* in the North Atlantic. *Global Biogeochem. Cycles*, **7,** 879–900.

Honjo, S. and R. A. Weller, 1997. Monsoon winds and carbon cycles in the Arabian Sea. *Oceanus*, **40**(2), 24–28.

Hughes, J. and T. Lamparter, 1999. Prokaryotes and phyochrome: the connection to chromophores and signalling. *Plant Physiol.*, **121,** 1059–1068.

IOCCG Report, Status and Plans for Satellite Ocean-Colour Missions: Considerations for Complementary Missions, 1999. *Report Number 2 of the International Ocean Colour Coordinating Group*, J. Yoder, ed. IOCCG, Dartmouth, Nova Scotia, Canada.

Jerlov, N. G., 1976. *Marine Optics*. Elsevier, Amsterdam.

Karentz, D., 1994. Ultraviolet tolerance mechanisms in Antarctic marine organisms. Ultraviolet radiation in Antarctica: measurements and biological effects. *Amer. Geophys. Union*, **62,** 93–110.

Karentz, D. and L. H. Lutze, 1990. Evaluation of biologically harmful ultraviolet radiation in Antarctica with a biological dosimeter designed for aquatic environments. *Limnol. Oceanogr.*, **35**(3), 549–561.

Karl, D. M., 1999. A sea of change: biogeochemical variability in the North Pacific Central Gyre, *Ecosystems*, **2,** 181–214.

Katz, M., D. Pak, G. Dickens and K. Miller, 1999. The source and fate of massive carbon input during the latest paleocene thermal maximum. *Science*, **286,** 1531–1533.

Kinkade, C. S., J. Marra, T. D. Dickey, C. Langdon, D. E. Sigurdson and R. Weller, 1999. Diel bio-optical variability observed from moored sensors in the Arabian Sea. *Deep-Sea Res. II*, **46,** 1813–1831.

Kirk, J. T. O., 1992. The nature and measurement of the light environment in the ocean. In *Primary Productivity and Biogeochemical Cycles in the Sea*, P. G. Falkowski, ed., Plenum Press, New York, pp. 9–29.

Kirk, J. T. O., 1994. *Light and Photosynthesis in Aquatic Ecosystems*, 2nd ed. Cambridge University Press, Cambridge.

Kok, B., 1956. On the inhibition of photosynthesis by intense light. *Biochim. Biophys. Acta*, **21,** 234–244.

Kolber, Z., J. Zehr and P. G. Falkowski, 1988. Effects of growth irradiance and nitrogen limitation on photosynthetic energy conversion in photosystem II. *Plant Physiol.*, **88,** 72–79.

Kolber, Z., K. D. Wyman and P. G. Falkowski, 1990. Natural variability in photosyntheetic energy conversion efficiency: a field study in the Gulf of Maine. *Limnol. Oceanogr.*, **35,** 72–79.

Kolber, Z. S., O. Prasil and P. Falkowski, 1998. Measurements of variable chlorophyll fluorescence using fast repetition rate techniques: defining methodology and experimental protocols. *Biochim. Biophys. Acta*, **1376,** 88–106.

Latimer, P. and E. Rabinowitch, 1959. Selective scattering of light by pigments in vivo. *Arch. Biochem. Biophys.*, **84,** 428–441.

Laws, E. A., P. G. Falkowski, et al., 2000. Temperature effects on export production in the open ocean. *Global Biogeochem. Cycles*, **14**(4), 1231–1246.

Lee, Z. P., K. L. Carder, S. K. Hawes, R. G. Steward, T. G. Peacock and C. O. Davis, 1994. A model for interpretation of hyperspectral remote-sensing reflectance. *Appl. Opt.*, **33,** 5721–5732.

Lee, Z. P., K. L. Carder, T. G. Peacock, C. O. Davis and J. Mueller, 1996. A method to derive ocean absorption coefficients from remote-sensing reflectance. *Appl. Opt.*, **35,** 453–462.

Lewis, M. R., 1987. Phytoplankton and thermal structure in the tropical ocean. *Oceanol. Acta*, Special Volume, 91–95.

Lewis, M. R., 1992. Satellite ocean color observations of global biogeochemical cycles. In *Primary Productivity and Biogeochemical Cycles in the Sea*, P. G. Falkowski and A. Woodhead, eds. Plenum Press, New York, pp. 139–154.

Lewis, M. R. and J. C. Smith, 1983. A small volume, short-incubation time method for measurement of photosynthesis as a function of incident irradiance. *Mar. Ecol. Prog. Ser.*, **13,** 99–102.

Lewis, M. R., J. J. Cullen and T. Platt, 1983. Phytoplankton and thermal structure in the upper ocean: consequences of non-uniformity in chlorophyll profile. *J. Geophys. Res.*, **88,** 2565–2570.

Lewis, M. R., W. G. Harrison, N. S. Oakey, D. Hebert and T. Platt, 1986. Vertical nitrate fluxes in the oligotrophic ocean. *Science*, **234,** 870–873.

Lewis, M. R., N. Kuring and C. Yentsch, 1988. Global patterns of ocean transparency: implications for the new production of the open ocean. *J. Geophys. Res.*, **93,** 6847–6856.

Lewis, M. R., M. E. Carr, G. C. Feldman, W. Esaias and C. McClain, 1990. Influence of penetrating solar radiation on the heat budget of the equatorial Pacific Ocean. *Nature*, **347,** 543–545.

Ley, A. C. and D. Mauzerall, 1982. Absolute absorption cross sections for photosystem II and the minimum quantum requirement for photosynthesis in Chlorella vulgaris. *Biochim. Biophys. Acta*, **680,** 95–106.

Long, S. P., S. Humpries, et al., 1994. Photoinhibition of photosynthesis in nature. *Ann. Rev. Plant Physiol. Plant Mol. Biol.*, **45,** 655-662.

Longhurst, A., S. Sathyendranath, et al., 1995. An estimate of global primary production in the ocean from satellite radiometer data. *J. Plankton Res.*, **17,** 1245–1271.

Madronich, S., R. L. McKenzie, M. M. Caldwell and L. O. Bjorn, 1995. Changes in ultraviolet radiation reaching the Earth's surface. *Ambio*, **24,** 143–152.

Mann, K. H. and J. R. N. Lazier, 1991. *Dynamics of Marine Ecosystems: Biological–Physical Interactions in the Oceans*. Blackwell Scientific Publications, Boston.

Marra, J., T. Dickey, W. S. Chamberlin, C. Ho, T. Granata, D. A. Kiefer, C. Langdon, R. Smith, R. Bidigare and M. Hamilton, 1992. Estimation of seasonal primary production from moored optical sensors in the Sargasso Sea. *J. Geophys. Res.*, **97,** 7399–7412.

Marra, J., T. D. Dickey, C. Ho, C. S. Kinkade, D. E. Sigurdson, R. A. Weller, and R. T. Barber, 1998. Variability in primary production as observed from moored sensors in the central Arabian Sea in 1995, *Deep-Sea Res. II*, **45,** 2253–2267.

McGillicuddy, D. J., A. R. Robinson, D. A. Siegel, H. W. Jannasch, R. Johnson, T. D. Dickey, J. D. McNeil, A. F. Michaels and A. H. Knap, 1998. New evidence for the impact of mesoscale eddies on biogeochemical cycling in the Sargasso Sea. *Nature*, **394,** 263–266.

McNeil, J. D., H. Jannasch, T. Dickey, D. McGillicuddy, M. Brzezinski and C. M. Sakamoto, 1999. New chemical, bio-optical, and physical observations of upper ocean response to the passage of a mesoscale eddy. *J. Geophys. Res.*, **104,** 15537–15548.

McPhaden, M. J., 1995. The Tropical Atmosphere–Ocean Array is completed. *Bull. Am. Meteorol. Soc.*, **76,** 739–741.

Milos, P. and J. W. Hastings, 1990. *Gonyaulax* proteins is at a translational level. *Naturwissenschaften*, **77,** 87–89.

Mitchell, J. M., 1976. An overview of climatic variability and its causal mechanisms. *Quat. Res.*, **6,** 481–493.

Mobley, C. D., 1994. *Light and Water: Radiative Transfer in Natural Waters*, Academic Press, San Diego, Calif.

Moore, C. C., J. R. V. Zaneveld and J. C. Kitchen, 1992. Preliminary results from in situ spectral absorption meter data. *Ocean Optics XI, SPIE*, **1750,** 330–337.

Morel, A., 1978. Available, usable, and stored radiant energy in relation to marine photosynthesis. *Deep-Sea Res.*, **25,** 673–688.

Morel, A., 1988. Optical modeling of the upper ocean in relation to biogenous matter content (case I waters). *J. Geophys. Res.*, **93,** 10749–10768.

Morel, A., 1991. Optics of marine particles. In *Particle Analysis in Oceanography*, S. Demers, ed. Springer-Verlag, Berlin, pp. 141–188.

Morel, A. and D. Antoine, 1994. Heating rate within the upper ocean in relation to its bio-optical state. *J. Phys. Oceanogr.*, **24,** 1652–1665.

Morel, A. and J.-F. Berthon, 1989. Surface pigments, algal biomass profiles, and potential production of the euphotic layer: relationships reinvestigated in view of remote-sensing applications. *Limnol. Oceanogr.*, **34,** 1545–1562.

Morel, A. and A. Bricaud, 1986. Inherent properties of algal cells including picoplankton: theoretical and experimental results. In *Photosynthetic Picoplankton*, T. Platt and W. K. W. Li, eds. pp. 521–559.

Mori, T., B. Binder and C. H. Johnson, 1996. Circadian gating of cell division in cyanobacteria growing with average doubling times of less than 24 hours. *Proc. Natl. Acad. Sci. USA*, **93**, 10183–10188.

Mulkidjanian, A. Y. and W. Junge, 1996. New photosynthesis or old. *Nature*, **379**, 304–305.

Neale, P. J., R. F. Davis and J. J. Cullen, 1998. Interactive effects of ozone depletion and vertical mixing on photosynthesis of Antarctic phytoplankton. *Nature*, **392**, 585–589.

Nelson, N. B., D. A. Siegel and A. F. Michaels, 1998. Seasonal dynamics of colored dissolved material in the Sargasso Sea. *Deep-Sea Res. I*, **34,** 931–957.

Neubauer, C., 1993. Multiple effects of dithiothreitol on nonphotochemical fluorescence quenching in intact chloroplasts—Influence on violaxanthin de-epoxidase and ascorbate perioxidase activity. *Plant Physiol.*, **103**(2), 575–583.

Ohlmann, J. C., D. A. Siegel and C. Gautier, 1996. Ocean mixed layer heating and solar penetration: a global analysis. *J. Climate*, **9,** 2265–2280.

Ohlmann, J. C., D. A. Siegel and L. Washburn, 1998. Radiant heating of the western equatorial Pacific during TOGA-COARE. *J. Geophys. Res.*, **103,** 5379–5395.

Olaizola, M., J. LaRoche, et al., 1994. Non-photochemical fluorescence quenching and the diadinoxathin cycle in a marine diatom. *Photosyn. Res.*, **41,** 357–370.

Olson, R. et al., 1990. Spatial and temporal distributions of prochlorophyte picoplankton in the North Atlantic Ocean. *Deep-Sea Res.*, **37,** 1033–1051.

Owens, T. G., P. G. Falkowski and T. E. Whiteledge, 1980. Diel periodicity in cellular chlorophyll content in marine diatoms. *Mar. Biol.*, **59,** 71–77.

Peixoto, J. P. and A. H. Oort, 1992. *Physics of Climate*. American Institute of Physics, New York.

Petrenko, A. A., B. H. Jones, T. D. Dickey, M. LeHaitre and C. Moore, 1997. Effects of a sewage plume on the biology, optical characteristics, and particle size distributions of coastal waters. *J. Geophys. Res.*, **102,** 25061–25071.

Platt, T. and S. Sathyendranath, 1991. Biological models as elements of coupled, atmosphere-ocean models for climate research. *J. Geophys. Res. C. Oceans,*, **96**(C2), 2585–2592.

Platt, T., P. Jauhari and S. Sathyendranath, 1992. The importance and measurement of new production, In *Primary Productivity and Biogeochemical Cycles in the Sea*, P. G. Falkowski and A. Woodhead, eds. Plenum Press, New York, pp. 273–284.

Pope, R. M. and E. S. Fry, 1997. Absorption spectrum (380–700 nm) of pure water. 2. Integrating cavity measurements. *Appl. Opt.*, **37,** 8710–8723.

Post, F., Z. Dubinsky, K. Wyman and P. G. Falkowski, 1985. Kinetics of light-intensity adaptation in a marine planktonic diatom. *Mar. Biol.*, **83,** 231–238.

Prasil, O., N. Adir and I. Ohad, 1992. Dynamics of photosystem II: mechanism of photoinhibition and recovery processes. In *The Photosystems: Structure, Function and Molecular Biology*, J. R. Barber, ed. Elsevier, New York, pp. 295–348.

Ramalho, C. B., J. W. Hastings and P. Colepicolo, 1995. Circadian oscillation of nitrate reductase activity in *Golyaulax polyedra* is due to changes in cellular protein levels. *Plant Physiol.*, **107,** 225–231.

Sarmiento, J. L., 1993. Ocean carbon cycle. *Chem. Eng. News*, **71,** 30–43.

Sathyendranath, S., A. D. Gouveia, S. R. Shetye, P. Ravindran and T. Platt, 1991. Biological control of surface temperature in the Arabian Sea. *Nature*, **349,** 54–56.

Schreiber, U. et al., 1993. PAM fluorometer based on medium-frequency pulsed Xe-flash measuring light: a highly sensitive new tool in basic and applied photosynthesis research. *Photosynthesis Res.*, **36,** 65–72.

Setlow, R. B., 1974. The wavelengths in sunlight effective in producing skin cancer: a theoretical analysis. *Proc. Nat. Acad. Sci. USA*, **71,** 3363–3366.

Siegel, D. A. and T. D. Dickey, 1987. On the parameterization of irradiance for ocean photoprocesses. *J. Geophys. Res.*, **92,** 14648–14662.

Siegel, D. A. and A. F. Michaels, 1996. Non-chlorophyll light attenuation in the open ocean: implications for biogeochemistry and remote sensing. *Deep-Sea Res. II*, **43,** 321–345.

Siegel, D. A., T. D. Dickey, L. Washburn, M. K. Hamilton and B. G. Mitchell, 1989. Optical determina-
tion of particulate abundance and production variations in the oligotrophic ocean. *Deep-Sea Res.*, **36,**
211–222.

Siegel, D. A., J. C. Ohlmann and L. Washburn, 1995. Solar radiation, phytoplankton pigments and radiant
heating of the equatorial warm pool. *J. Geophys. Res.*, **100,** 4885–4891.

Simonot, J. Y. and H. LeTreut, 1986. A climatological field of mean optical properties of the world ocean.
J. Geophys. Res., **91,** 6642–6646.

Simpson, J. J. and T. D. Dickey, 1981a. Alternative parameterizations of downward irradiance and their
dynamical significance. *J. Phys. Oceanogr.*, **11,** 876–882.

Simpson, J. J. and T. D. Dickey, 1981b. The relationship between downward irradiance and upper ocean
structure. *J. Phys. Oceanogr.*, **11,** 309–323.

Smith, R. C. and K. Baker, 1978. The bio-optical state of ocean waters and remote sensing. *Limnol.
Oceanogr.*, **11,** 309–323.

Smith, R. C. and K. S. Baker, 1981. Optical properties of the clearest natural waters. *Appl. Opt.*, **20,**
177–184.

Smith, R. C., K. J. Waters and K. S. Baker, 1991. Optical variability and pigment biomass in the Sargasso
Sea as determined using deep sea optical mooring data. *J. Geophys. Res.*, **96,** 8665–8686.

Smith, R. C., B. B. Prezelin, et al., 1992. Ozone depletion: ultraviolet radiation and phytoplankton biology
in Antarctic waters. *Science*, **255,** 952–959.

Smith, S. L., L. A. Codispoti, J. M. Morrison and R. T. Barber, 1998. The 1994–1996 Arabian Sea
Expedition: an integrated, interdisciplinary investigation of the response of the northwestern Indian
Ocean to monsoonal forcing. *Deep-Sea Res. II*, **45,** 1905–1916.

Spinrad, R. W., K. L. Carder and M. J. Perry, 1994. *Ocean Optics*. Oxford University Press, Oxford.

Stramska, M. and T. D. Dickey, 1992a. Short-term variations of the bio-optical properties of the ocean
in response to cloud-induced irradiance fluctuations. *J. Geophys. Res.*, **97,** 5713–5721.

Stramska, M. and T. D. Dickey, 1992b. Variability of bio-optical properties in the upper ocean associated
with diel cycles in phytoplankton population. *J. Geophys. Res.*, **97,** 17873–17887.

Stramska, M. and T. Dickey, 1993. Phytoplankton bloom and the vertical thermal structure of the upper
ocean. *J. Mar. Res.*, **51,** 819–842.

Stramska, M. and T. Dickey, 1994. Modeling phytoplankton dynamics in the northeast Atlantic during
the initiation of the spring bloom. *J. Geophys. Res.*, **99,** 10241–10253.

Stramska, M. and T. D. Dickey, 1998. Short term variability of the underwater light field in the olig-
otrophic ocean in response to surface waves and clouds. *Deep-Sea Res. I*, **45,** 1393–1410.

Stramski, D. and D. A. Kiefer, 1991. Light scattering by microorganisms in the open ocean. *Prog.
Oceanogr.*, **28,** 343–383.

Stramski, D., A. Shalapyonok and R. A. Reynolds, 1995. Optical characterization of the oceanic unicel-
lular cyanobacterium *Synechococcus* grown under a day–night cycle in natural irradiance. *J. Geophys.
Res.*, **100,** 13295–13307.

Sverdrup, H. U., 1953. On the conditions for vernal blooming of phytoplankton. *J. Cons. Perm. Int.
Explor. Mer.*, **18,** 287–295.

Takahashi, J. S., 1992. Circadian clock genes are ticking. *Science*, **258,** 238–240.

Twardowski, M. S., J. M. Sullivan, P. L. Donaghay and J. R. V Zaneveld, 1999. Microscale quantification
of the absorption by dissolved and particulate material in coastal waters with an ac-9. *J. Atmos. Ocean.
Technol.*, **16,** 691–707.

Tyrell, T., P. M. Holligan and C. D. Mobley, 1999. Optical impacts of oceanic coccolithophore blooms.
J. Geophys. Res., **104,** 3223–3241.

van de Hulst, H. C., 1981. *Light Scattering by Small Particles*. Dover Publications, New York.

Vaulot, D. and F. Partensky, 1992. Cell cycle distributions of prochlorophytes in the northwestern
Mediterranean Sea. *Deep-Sea Res.*, **39,** 727–742.

Vincent, W. F. and S. Roy, 1993. Solar ultraviolet-B radiation and aquatic primary production: damage,
protection and recovery. *Environ. Rev.*, **1,** 1–12.

Vodacek, A., N. V. Blough, M. D. DeGrandpre, E. T. Peltzer and R. K. Nelson, 1997. Seasonal varia-

tion of CDOM and DOC in the Middle Atlantic Bight: terrestrial inputs and photooxidation. *Limnol. Oceanogr.*, **42,** 674–686.

Volk, T. and M. I. Hoffert, 1985. Ocean carbon pumps: analysis of relative strengths and efficiencies in ocean-driven atmospheric CO_2 exchanges. In *The Carbon Cycle and Atmospheric CO_2: Natural Variations Archean to Present*, E. T. Sunquist and W. S. Broeker, eds. American Geophysical Union, Washington, D.C., pp. 99–110.

Weller, R. A., M. F. Baumgartner, S. A. Josey, A. S. Fischer and J. C. Kindle, 1998. Atmospheric forcing in the Arabian Sea during 1994–1995; observations and comparisons with climatology and models, *Deep-Sea Res. II*, **45,** 1961–1999.

Wells, N., 1997. *The Atmosphere and Ocean: A Physical Introduction*, 2nd ed. Wiley, New York.

Wiggert, J. D., T. D. Dickey and T. C. Granata, 1994. The effect of temporal undersampling on primary production estimates. *J. Geophys. Res.*, **99,** 3361–3371.

Wiggert, J., B. Jones, T. Dickey, K. Brink, R. Weller, J. Marra and L. Codispoti, 2000. The northeast monsoon's impact on mixing, phytoplankton biomass, and nutrient cycling in the Arabian Sea. *Deep-Sea Res. II*, **47,** 1353–1385.

Woods, J. D. and W. Barkmann, 1986. The response of the upper ocean to solar heating. I. The mixed layer. *Q. J. R. Meteorol. Soc.*, **112,** 1–27.

Woods, J. D., W. Barkmann and A. Horch, 1984. Solar heating of the oceans: diurnal, seasonal, and meridional variation. *Q. J. R. Meteorol. Soc.*, **110,** 633–656.

Yentsch, C. S., 1960. The influence of phytoplankton pigments on the colour of sea water, *Deep-Sea Res.*, **7,** 1–9.

Yentsch, C. S., 1980. Phytoplankton growth in the sea, a coalescence of disciplines. In *Primary Productivity in the Sea*, P. G. Falkowski, ed. Plenum Press, New York, pp. 17–31.

Yoder, J. A., S. G. Ackleson, R. T. Barber, P. Flament, and W. M. Balch, 1994. A line in the sea. *Nature*, **371,** 689–692.

Zaneveld, J. R. V. and R. W. Spinrad, 1980. An arctangent model of irradiance in the sea. *J. Geophys. Res.*, **85,** 4919–4922.

Zepp, R. G., T. V. Callaghan and D. J. Erickson, 1998. Effects of enhanced solar ultraviolet radiation on biogeochemical cycles. *J. Photochem. Photobiol. B: Biol.*, **46,** 69–82.

Zhang, X., M. R. Lewis and B. Johnson, 1998. The influence of bubbles on scattering of light in the ocean. *Appl. Opt.*, **37,** 6525–6536.